

See discussions, stats, and author profiles for this publication at: <https://www.researchgate.net/publication/263940479>

Production characteristics of the steam-assisted gravity drainage (SAGD) and solvent-aided SAGD (SA-SAGD) processes using a 2-D macroscale physical model. ACS J Energy Fuels

ARTICLE *in* ENERGY & FUELS · JULY 2012

Impact Factor: 2.79 · DOI: 10.1021/ef300354j

CITATIONS

4

READS

40

3 AUTHORS, INCLUDING:



Omidreza Mohammadzadeh

University of Waterloo

15 PUBLICATIONS 101 CITATIONS

[SEE PROFILE](#)



Ioannis Chatzis

University of Waterloo

116 PUBLICATIONS 2,580 CITATIONS

[SEE PROFILE](#)

Pore-Level Investigation of Heavy Oil and Bitumen Recovery Using Solvent – Aided Steam Assisted Gravity Drainage (SA-SAGD) Process

O. Mohammadzadeh,* N. Rezaei, and I. Chatzis

Department of Chemical Engineering, University of Waterloo, Waterloo, Ontario N2L 3G1, Canada

Received May 18, 2010. Revised Manuscript Received September 18, 2010

Attempts have been made to reduce the energy requirements of steam assisted gravity drainage (SAGD) projects through coupled thermal and solvent processes (i.e., hybrid SAGD). The augmented process brings superior features to the SAGD process in terms of reduced energy requirement, enhanced produced oil quality, and also improved oil recoveries. The pore-level recovery mechanisms of the hybrid SAGD process have not been investigated yet. The main objective of this paper is to visually investigate and to document the pore-scale events during the hybrid SAGD process using glass micromodel type of porous media. Different additives (*n*-pentane and *n*-hexane) were added to steam prior to injecting into the models. Experiments were conducted in an inverted-bell vacuum chamber to reduce the excessive heat loss to the surroundings. The results indicate that the gravity drainage process takes place through a layer of pores composed of 1–5 pores in thickness, in the direction perpendicular to the nominal oil–gaseous mixture interface, in the mobilized region. The interplay between gravity and capillary forces results in the drainage of the mobilized oil. The visualization results demonstrated the coexistence of water-in-oil and solvent-in-water emulsification at the interface because of the local condensation of both steam and the vaporized solvent. The extent of emulsification depends directly on the temperature gradient between the gaseous mixture and the mobile oil phase. Asphaltene precipitation was also observed when the condensed solvent reached the bitumen interface. As the nature of the process involves partially miscible displacements, the extent of film-flow drainage of the mobilized oil was also significant. Other pore-scale phenomena include localized entrapment of steam and vaporized solvent followed by condensation, snap-off of liquid films, steam and solvent vapor condensation at the interface because of the temperature gradient and capillary instabilities.

Introduction

Increasing energy consumption and continuous depletion of hydrocarbon reservoirs will result in a conventional oil production peak in the near future. Thus, the gap between the global conventional oil supplies and the required amount of fossil fuel energy will grow. Extensive attempts were made during the last two decades to fill this gap, especially using innovative emerging heavy and extra-heavy oil and bitumen production technologies. Most of these recovery methods have been developed in Canada, considering the fact that Canada and Venezuela have the largest deposits of heavy oil and bitumen throughout the world. The horizontal well drilling technology opened a new horizon for the recovery of heavy and extra-heavy oil. Most of the in situ upgrading recovery techniques, including the steam assisted gravity drainage (SAGD) recovery method, take advantage of horizontal injection and production wells. In these recovery processes, the vacated pores in the reservoir are filled mainly either with steam or with a gaseous mixture of steam and solvent in the case of SAGD and solvent aided SAGD (SA-SAGD) recovery methods, respectively. The use of long horizontal wells combined with the reduced viscosity of the produced oil allows economic production with limited amount of bypassed residual oil in the invaded region.

The basic concept behind the SAGD process is that if steam is injected through a horizontal injector which is completed above but close to the horizontal producer, the steam phase tends to rise while the condensates together with the heated oil

flow under the action of gravity. The draining liquids should be removed continuously from the production well to avoid accumulation of the mobilized oil at the proximity of the wells. Figure 1 shows a schematic of a vertical cross-section in typical SAGD process, perpendicular to the horizontal extension of the paired wells. In the SAGD process, the oil viscosity is lowered using steam injection. High final recovery values as well as economical oil production rates are achievable using this recovery technique based on the extensive laboratory and field trials; however, there are still some issues related to the high energy intensity of the process, excessive thermal energy losses within the reservoir, CO₂ generation, and expensive surface water treatment facilities.^{1–5}

Considering the drawbacks of the conventional SAGD process, some modifications and even alternative recovery processes were proposed to enhance the overall performance of the SAGD process such as the use of noncondensable gas along with the injected steam phase (SAGP¹³) to reduce the amount of heat loss to the overburden and also low-pressure SAGD.⁶ On the other hand, an alternative solvent-based

(1) Butler, R. M.; McNab, G. S.; Lo, H. Y. *Can. J. Chem. Eng.* **1981**, 59, 455–460.

(2) Butler, R. M. Stephens, D. J. *J. Can. Pet. Tech.* **1981**, April–June No. paper no. 81–02–07.

(3) Butler, R. M. *J. Can. Pet. Tech.* **1998**, 37, 7.

(4) Butler, R. M. *J. Can. Pet. Tech.* **2001**, 40, 1.

(5) Al-Bahlani, A. M.; Babadagli, T. *J. Pet. Sci. Eng.* **2009**, 68, 135–150.

(6) Jiang, Q.; Butler, R. M.; Yee, C. T. In *The Steam and Gas Push (SAGP)-2: mechanism analysis and physical model testing*, Proceedings of the Petroleum Society 49th Annual Technical Meeting, Calgary, Alberta, Canada, June 8–10, 1998; paper 98–43.

*Corresponding author. E-mail: omohamma@uwaterloo.ca.

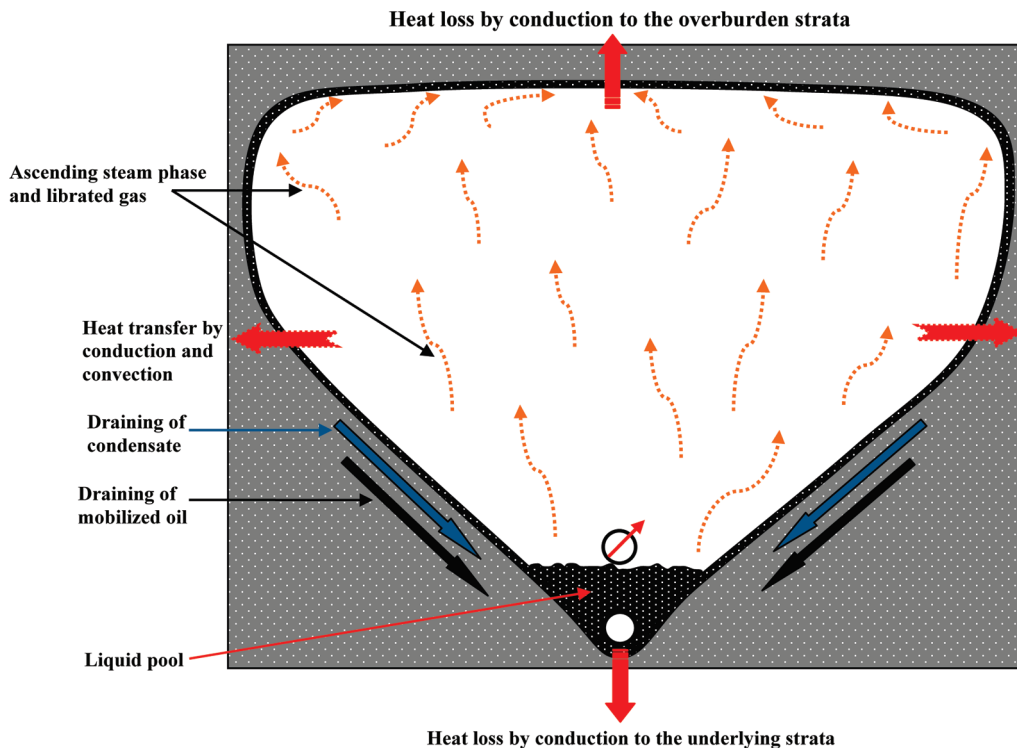


Figure 1. Conceptual flow diagram of the SAGD process.

recovery method called the VAPEX process was proposed. In the VAPEX process, a hydrocarbon solvent is injected at a pressure below the dew point into the oil layer instead of the steam. It is evident that mass transfer by diffusion, the mechanism responsible for the dilution of bitumen to reduce its viscosity in the conventional VAPEX process, is much slower than the thermally induced viscosity reduction achieved in the case of the SAGD process. The VAPEX process suffers from lower oil production rates compared to the SAGD process. However, this process could be beneficial because of the lower energy requirement, lower CO₂ emissions, possible in situ upgrading, and minimizing the cost of water treatment.⁷

One modification of the SAGD process uses the idea of adding some steam additives to the injected stream in order to further reduce the bitumen's viscosity as well as to lower SAGD's energy cost. This method, the so-called solvent aided SAGD

(i.e., SA-SAGD) process has been extensively studied in the literature under different commercial names.^{8–12,14–23} The SA-SAGD processes offer the combined advantages of a conventional SAGD and a conventional VAPEX process by reducing the inherent bitumen viscosity with the aid of solvent dilution and steam heating. Other advantages of the hybrid SAGD processes include increased recovery potential compared to that of the VAPEX process, reduced energy requirements compared to that of the SAGD process, and possibly in situ upgrading.

Although the SAGD process is acknowledged as one of the main heavy oil recovery techniques, no extensive efforts had been made in the published literature to critically study the pore-scale aspects of this process. Considering the fact that major macroscale characteristics of a pilot-scale or field-scale SAGD process depend on the pore-scale aspects of the process, attempts have been made recently to investigate some of

- (7) Butler, R. M.; Mokrys, I. J. *J. Can. Pet. Tech.* **1991**, *30*, 1.
- (8) Nasr, T. N.; Isaacs, E. E. Process for enhancing hydrocarbon mobility using a steam additive. US Patent 6,230,814, May 15, 2001.
- (9) Nasr, T. N.; Beaulieu, G.; Golbeck, H.; Heck, G. *J. Can. Pet. Tech.* **2003**, *42*, 1.
- (10) Nasr, T. N.; Ayodele, O. R. Thermal techniques for the recovery of heavy oil and bitumen. *SPE International IOR Conference Asia Pacific*, Kuala Lumpur, Malaysia, Dec 5–6, 2005; SPE paper 97488.
- (11) Nasr, T. N.; Beaulieu, G.; Golbeck, H.; Heck, G. Novel Expanding Solvent-SAGD process (ES-SAGD). *Petroleum Society's Canadian International Petroleum Conference*, Calgary, Alberta, Canada, June 11–13, 2002; paper no. 2002-072.
- (12) Nasr, T. N.; Kimber, K. D.; Vendrinsky, D. A.; and Jha, K. N. Process enhancement in horizontal wells through the use of vertical drainage channels and hydrocarbon additives. *Western Regional Meeting*, Long Beach, CA, March 20–22, 1991; SPE paper 21794.
- (13) Butler, R. M. The Behavior of Non-condensable Gas in SAGD – A Rationalization. *Petroleum Society's Canadian International Petroleum Conference*, Petroleum Society Paper No.: 2002-117, Calgary, Alberta, Canada, June 11–13.
- (14) Zhao, L. Steam Alternating Solvent process; *SPE International Thermal Operations and Heavy Oil Symposium and Western Regional Meeting*, Bakersfield, CA, March 16–18, 2004, SPE paper 86957.
- (15) Zhao, L.; Nasr, T. N.; Haung, H.; Beaulieu, G.; Heck, G.; Golbeck, H. *J. Can. Pet. Tech.* **2005**, *44*, 9.
- (16) Gupta, S.; Gittins, S.; and Picherack, P. Field implementation of Solvent Aided Process, *Petroleum Society's Canadian International Petroleum Conference*, Calgary, Alberta, Canada, June 11–13, 2002.
- (17) Gupta, S.; Gittins, S.; Picherack, P. *J. Can. Pet. Tech.* **2003**, *43*, 2.
- (18) Gupta, S.; Gittins, S.; Picherack, P. *J. Can. Pet. Tech.* **2005**, *44*, 11.
- (19) Gupta, S. C.; Gittins, S. D. Christina Lake Solvent Aided Process pilot. *Petroleum Society's Canadian International Petroleum Conference*, Calgary, Alberta, Canada, June 7–9, 2005.
- (20) Gupta, S. C.; Gittins, S. D. *J. Can. Pet. Tech.* **2006**, *45*, 9.
- (21) Gupta, S. C.; Gittins, S. D. Effect of solvent sequencing and other enhancements on Solvent Aided Process. *Petroleum Society's 7th Canadian International Petroleum Conference (57th Annual Technical Meeting)*, Calgary, Alberta, Canada, June 13–15, 2006.
- (22) Boyle, T. B.; Gittins, S. D.; Chakrabarty, C. *J. Can. Pet. Tech.* **2003**, *42*, No. paper number 2002-300.
- (23) McCormack, M. E. Design of steam-hexane injection wells for gravity drainage systems. *Petroleum Society's 8th Canadian International Petroleum Conference (58th Annual Technical Meeting)*, Calgary, Alberta, Canada, June 12–14, 2007; paper no. 2007-102.

the microscale aspects of the process using visualization techniques.^{24,25} Glass-etched micromodels were selected to visualize the pertaining pore-level recovery mechanisms of the mobilized oil, as well as to document the microscale aspects of the process. According to the qualitative results of the flow visualization, it was found that two simultaneous pore-level recovery mechanisms are responsible for the drainage of the thermally mobilized oil, namely capillary drainage displacement as well as film-flow drainage displacement mechanisms. The steam chamber propagation behavior was found to be influenced by the randomly distributed fingering nature of the unstable invading steam front near the mobilized oil–steam chamber interface (i.e., a region of a few pores near the nominal bitumen-filled pores that attain mobility which is called the mobilized region). The extent of steam fingering phenomena was seen to be severe during the vertical growth stage of the steam chamber where the buoyant front of the steam phase is protruding through the pores containing a continuum of cold bitumen, especially near the topside of the steam chamber. The steam fingering phenomena were also observed during the outward propagation of the steam chamber at the proximity of its side wings. Simultaneous cocurrent and countercurrent flow of different acting phases were observed near the lateral sides of the steam chamber, which are responsible for the horizontal expansion of the invaded region. Several fluid flow regions were demonstrated in a typical expanding SAGD pattern in which different acting phases (i.e., steam, draining condensate, and mobilized oil) flow under the action of primarily gravity and capillary forces. These visualization experiments helped us to determine the approximate thickness of these flow zones and to understand the drainage behavior and fluid flow regimes of different fluid phases within each particular pore-level fluid zone under the pertaining experimental conditions. In addition, several interfacial regions associated with these flow zones were also defined and characterized at the pore-level. The emulsification phenomenon, which is an important characteristic of a typical SAGD process at the pore-scale, was also hypothesized to be interpreted by the interfacial thermodynamic approach of non-spreading characteristics of water over oil in the presence of a gaseous phase. This approach, which is based on the entrapment process of the water condensate droplets within the continuum of the draining mobilized oil, was also experimentally verified using this pore-scale study of the SAGD process. It is believed that these findings, along with the detailed quantitative analysis of the process performance, could improve our understanding about the relevant physics of the process, which in turn could have a profound effect on the development of realistic modeling procedures of the noted process.

As the overall scheme of the SA-SAGD type of process is quite similar to that of the SAGD process in terms of the injection and production patterns, vapor chamber growth, and fluid flow concepts in porous media, it is believed that the previously employed experimental methodology could also be used to qualitatively and quantitatively investigate the pore-level aspects of the SA-SAGD process. In this paper, we aim to document and to systematically describe the pore-level aspects of the SA-SAGD process using visualization experiments, with

(24) Mohammadzadeh, O.; Chatzis, I. Pore-level Investigation of Heavy Oil Recovery using Steam Assisted Gravity Drainage (SAGD). *International Petroleum Technology Conference*, Doha, Qatar, December 7–9, 2009; IPTC paper number 13403.

(25) Mohammadzadeh, O.; Chatzis, I. *Oil Gas Sci. Technol.–Rev. IFP* 2010, 65, 435–444.

more emphasis on the qualitative microlevel mass transfer features of the process. As the pertaining mass transfer aspects of the SA-SAGD process were the main reason for proposing such a heavy oil recovery technique, the essence of this paper was decided to be the documentation of the transport phenomena of this process at the pore-level. Specific design of our SAGD and SA-SAGD visualization experiments enabled us to qualitatively and quantitatively analyze the heat transfer aspects of these two processes at the pore-scale in terms of describing the governing heat transfer mechanisms, as well as contouring the temperature distribution through entire pore-level flow regions. It was generally found that the heat transfer physics of the SA-SAGD process is within the same context of that of the SAGD process. However, it is worthwhile to note that qualitative heat-transfer-based descriptions are pointed out frequently in the current article whenever their use was beneficial to articulate the pore-scale physics of the process. Direct visualization experiments using glass micromodel type of porous media were selected in order to study the pore-scale aspects of the SA-SAGD process. Pore-scale events were recorded using digital photo capturing techniques as well as continuous real-time video recording. The snapshots were analyzed using image processing.

Literature Review of SA-SAGD Processes

It was believed that coinjection or alternate injection of a solvent along with steam could be an appropriate alternative for steam-based processes. The idea of solvent additives in steam injection was introduced by Farouq Ali and Abad.²⁷ Mokrys and Butler²⁸ compared the performance of the SAGD process with that of the SA-SAGD process and concluded that use of propane resulted in 30% reduction in steam requirements. They also recovered about 99% of the injected propane at the end of the SA-SAGD process through the blow-down stage. Use of propane as the light hydrocarbon additive in the steam phase was well-studied in the literature.^{29–32} According to these studies, a preliminary start-up stage was conducted in which superheated steam injection resulted in creation of a limited hot region, especially at the proximity of the injection well. This preliminary injection procedure reduced the start-up duration of the process. Steam and propane were then coinjected which resulted in enhanced production performance and reduced energy requirements of the solvent-aided process. Considering general aspects of the typical SA-SAGD processes, including solvent selection criteria, operational conditions, and injection scheme, these hybrid SAGD processes could be divided into three main categories which are briefly described in this section:

(26) James, L. A. Mass Transfer Mechanisms during the Solvent Recovery of Heavy Oil, Ph.D. Thesis 2009, University of Waterloo, Waterloo, ON, Canada.

(27) Farouq Ali, S. M.; Abad, B. *J. Can. Pet. Tech.* 1976, No. July–September, 80–90.

(28) Mokrys, I. J.; Butler, R. M. In *In-Situ Upgrading of Heavy Oil and Bitumen by Propane De-asphalting: The VAPEx Process*. *Production Operations Symposium*, Oklahoma City, March 1993, SPE 25452.

(29) Gotie, J. G.; Mamora, D. D.; Ferguson, A. M. *Experimental study of Morichal heavy oil recovery using combined steam and propane injection*; 2001, SPE 69566.

(30) Mamora, D. D.; Rivero, J. A.; Hendroyono, A.; Venturini, G. J. *Experimental and simulation studies of steam-propane injection for the Hamaca and Duri fields*; 2003, SPE 84201.

(31) Ferguson, M. A.; Mamora, D. D.; Goite, J. G. *Steam-propane injection for production enhancement of heavy Morichal oil*; 2001, SPE 69689.

(32) Rivero, J. A.; Mamora, D. D. *Production acceleration and injectivity enhancement using steam-propane injection for Hamaca extra-heavy oil*; 2002, SPE 75129.

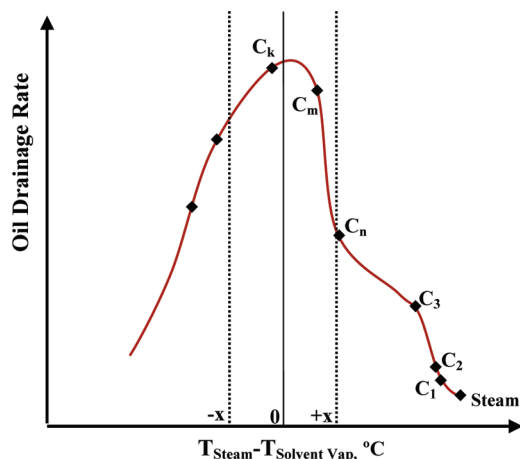


Figure 2. Schematic representation of the ES-SAGD process performance as a function of the vaporization temperature difference. Adapted from refs 9 and 11.

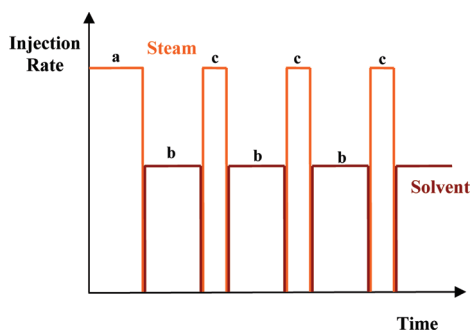


Figure 3. SAS injection process pattern. Adapted from ref 14.

(a) Expanding Solvent Steam Assisted Gravity Drainage (ES-SAGD). This method was proposed and patented by Nasr et. al^{8–12} as a modification to the conventional SAGD method. This process was successfully field tested and the results were promising in enhancing the oil to steam ratio (OSR) and recovery rates, thus reducing the energy intensity and water requirements compared to a conventional SAGD process. In this recovery technique, a small concentration of condensable hydrocarbon additive is coinjected along with the steam phase through a conventional SAGD pattern. There are some screening criteria to select the suitable solvent: for example, its vaporization temperature should match that of the steam phase at the operating chamber pressure. The higher the solvent carbon number is, the higher the vaporization temperature would be. This allows operators to select the appropriate steam additive among the hydrocarbon solvents. The steam additive should be kept in the gaseous state when traveling from the injection well until it reaches the bitumen surface. Experimental and numerical simulation studies performed by Nasr et. al^{8–12} proved that as the condensable hydrocarbon solvent becomes of heavier molecular weight, the resulting recovery performance is better; however, there is a local maxima in the production performance curve of the ES-SAGD process as schematically demonstrated in Figure 2. In this figure, oil drainage rates are schematically plotted as a function of the difference between steam temperature and solvent vaporization temperature. It is evident that the lower the temperature difference, the more effective the added solvent. Solvents whose vaporization temperatures locate their nominal position on the curve between the two vertical dotted lines in Figure 2 seem to be more effective

than the others. Thus the temperature difference range of the $(-x)$ to $(+x)$ °C could be considered as the favorable “ ΔT_{vap} ” for the solvent and the steam phases in the ES-SAGD process.

(b) Steam Alternating Solvent (SAS) Process. The SAS process involves the alternate injection of the steam and the solvent phases using the same well configuration as that of the SAGD process. The idea is to replace the large amounts of steam injection in the SAGD process with solvent injection. Higher oil production rates with lower energy requirements can be achieved using this recovery scheme. The dew point temperature of the solvent should be somewhere between the initial reservoir temperature and the steam temperature. According to the schematic diagram of the SAS process presented in Figure 3, this process has a cyclic nature, starting with a certain start-up period (part a). The steam injection period (part c) will continue until the heat loss to the surrounding starts to increase, and then, it is followed up by the solvent injection cycle (part b). The solvent injection cycles would then be stopped to prevent further temperature drop in the chamber. The overall performance of the SAS process was verified with both experimental and simulation studies.^{14,15} Experimental studies of the SAS process revealed that this process results in lower average oil production rates than those of the analogous SAGD process. However, numerical simulation results revealed that it is feasible to achieve average oil production rates and cumulative oil production comparable with, or even higher than those of the conventional SAGD process. This is due to the enhanced mobility of the live oil attained at the interfacial region in the SAS process compared to that of the conventional SAGD process. Although the mobilized oil viscosity is lower in the conventional SAGD compared to that of the SAS process, the oil relative permeability is more enhanced in the SAS process as a result of substantially lower water saturation compared to the conventional SAGD process.

Numerical simulation results showed that only a portion of the swept area of the SAS process is at the steam temperature and there are significant temperature variations within the depleted region.^{14,15} The presence of temperature distribution irregularities within the invaded area of a SA-SAGD process was also observed during the course of our visualization experiments. Although some localized spots within the invaded area reach the injection temperature in a typical SA-SAGD process, especially during the outward encroachment of the chamber, there were still significant temperature gradients near the mobilized region. Due to this sharp temperature gradient across the interfacial region of the SA-SAGD process, which is in the order of 30–40 °C in magnitude obtained from our visualization experiments under prevailing operational conditions, the solvent content of the injected phase tends to move ahead of the steam phase and condense over the bitumen surface based on its lower dew point temperature compared to that of the steam. It is also possible to experience some pore-level temperature gradients even through the invaded area as a result of the presence of the bypassed oil region, the presence of clogged pores with precipitated asphaltene, localized entrapment of the water condensate ahead of the mobilized region, and the heat loss from the invaded region to the surrounding environment.

(c) Solvent Aided Process (SAP). The main purpose of this process is to add small amounts of light hydrocarbon solvent (such as propane or butane) into the steam phase in a conventional SAGD configuration and use the combined effects of solvent dilution along with the thermal heating. The injection procedure is initiated with the conventional SAGD

Table 1. Physical and Pore-Scale Characteristics of the Micromodels

model name	DC1	DL1	OM1	OM2
physical dimensions				
length (mm)	304.00	304.00	301.00	301.00
pattern length (no. of pores)	190	149	150	150
width (mm)	141.00	100.00	101.00	101.00
pattern width (no. of pores)	89	49	50	50
pore-scale dimensions				
depth of etching ^a (μm)	127.70 ± 0.80	250.20 ± 0.90	118.90 ± 1.70	196.80 ± 6.60
pore body width (mm)	1.31	2.04	2.00	2.00
pore throat width (mm)	0.49	0.67	0.30	0.30
particle size (mm)	1.11	0.99	1.20	1.20

^a Depth of etching at the pore body space.

start-up phase in which steam is circulated through the horizontal well pair. Co-injection of the steam–solvent mixture is started after expiry of a certain initial period in the life of the normal SAGD cycle, first to commence an initial communication between the paired horizontal wells and second to allow for the development of initial steam chamber. The solvent–steam mixture should be injected in the vapor state with sufficient thermal energy content such that most of the solvent in the chamber remains in the vapor phase as it moves with the steam phase toward the condensation front. Although some other solvent-aided modifications of the SAGD process enhance its overall performance, it seems that SAP performance is better in comparison, based on the numerical simulation studies as well as field implementation of the process.^{16–23} There are some limitations in other modifications of the SAGD and VAPEX processes, which challenge their technical merits as well as their economic viability. For example, in the case of the ES-SAGD process, it was suggested that a hydrocarbon solvent (or a mixture of solvents), whose condensation characteristics match that of the steam phase at the operating conditions, is coinjected with the steam phase. However, a simple, light hydrocarbon solvent could be used in the SAP instead of expensive solvent mixtures, without any need to match the condensation–vaporization characteristics of the solvent and the steam phases. Moreover, it is unnecessary to support the chamber pressure with a non-condensable gas in the SAP as it is required in some variations of the VAPEX process. The SAP was successfully field tested and promising results regarding the increased production rates as well as reduced steam requirements compared to those of the conventional SAGD process were achieved based on the pilot tests and the numerical simulations.^{16–20} Numerical simulation studies showed that higher production rates could be achieved using lighter hydrocarbon solvents and also larger solvent to steam ratios at the injection side. In addition, the lighter the solvent and the higher its concentration, the lower the energy intensity of the SAP.^{16–20}

Experimental Setup and Model Preparation for the SA-SAGD Visualization Experiments

Glass-etched micromodels with detailed characterized pore structures were employed to conduct the SA-SAGD visualization experiments. The etched porous patterns were fully characterized in terms of physical dimensional properties as well as detailed pore-scale characteristics. The pore-level characterization is used for further quantitative pore-scale analysis which is not part of

this paper. A summary of the micromodels' characteristics and porous pattern properties is presented in Table 1. The main purpose of this paper is to mechanistically investigate the pore-scale aspects of the SA-SAGD process. It is evident that the quantitative results obtained using 2D micromodel of porous media cannot be extended to the real case 3D porous structure where pores are more interconnected. The extent of film flow, as well as the pore interconnectedness, is higher in the three-dimensional space of the porous media compared to that of the two-dimensional pore network framework where bicontinua of two phases cannot exist simultaneously.

A close-up of one of the employed glass micromodels, saturated with bitumen, is presented in Figure 4a. A line-source scheme of injection and point-source production was designed for the micromodels to facilitate the early development of the vapor chamber. As a result, these experiments represent the lateral encroachment period of the vapor chamber. Thanks to the symmetry of the geometrical pattern of a typical SA-SAGD process, a high permeable trough was designed at one side of the etched pattern to experimentally simulate only half of the process scheme. This ditch-like channel or trough, which is relatively large in size and hence in permeability compared to the pores, was made along the entire height of the model adjacent to the pore network, simulating a vertical line source of gaseous mixture injection (i.e., left side of the micromodel in Figure 4a which is covered entirely by strips of aluminum foil). A production hole was drilled at the bottom of the trough to facilitate the gravity drainage process, providing sufficient drainage height above it. Each micromodel was secured in a model holder and then was placed vertically to attain the gravity-dominated flow scheme. Each micromodel was first saturated with Cold Lake bitumen in a convection oven at a temperature of 60 °C using a syringe pump. The bitumen-filled micromodel was then brought to room environment to represent the initial experimental conditions ($T \approx 23^\circ\text{C}$).

A steam and solvent vapor generation and injection system was used to play the role of injection supply facilities. All the tubing connections were either heated or insulated to provide a gaseous mixture of steam and solvent under superheated conditions and also to avoid the injected gaseous mixture from being condensed within the transfer lines. Liquid water and liquid solvent phases were pumped using a high-precision, low discharge rate FMI LAB pump (Models RP-G400 and RP-SY) and an ISCO pump accordingly. A band heater and a coil heater, whose input powers were set based on the volumetric pumping rates of the liquids in such a way to generate superheated vapor state at their outlet lines, were used to generate the gaseous phases. The superheated steam and superheated solvent vapor were then mixed together in an injection line while being heated to maintain the superheating state of the gaseous mixture. The micromodel was then connected to the supply flow line of the superheated gaseous mixture at the injection spot. The gaseous mixture was allowed to enter the micromodel at the top and to fill the trough all the way down on one side of the pore network. In order to mobilize the oil phase within the pores adjacent to the trough, applying a start-up procedure was required. Only steam phase was injected through the injection line and it was then produced directly from the production end. This procedure involves introduction of the fresh steam phase to the pores attached to the injection trough, which initializes the mobilization process of the viscous oil. The production metering valve was then closed to avoid any steam breakthrough from the production port. Injecting the solvent vapor into the steam injection line was then started and continued up until the end of the SA-SAGD process. To avoid any gaseous mixture from escaping out of the micromodel, a finite head of the drained liquids (i.e., condensed steam at the beginning and drained emulsions, condensed steam, and mobilized live oil afterward) was maintained continuously inside the $1/8$ in. Teflon tube production line to prevent gaseous phase breakthrough. This column of the drained liquid was emptied occasionally using the production metering valve. Visualization experiments of the

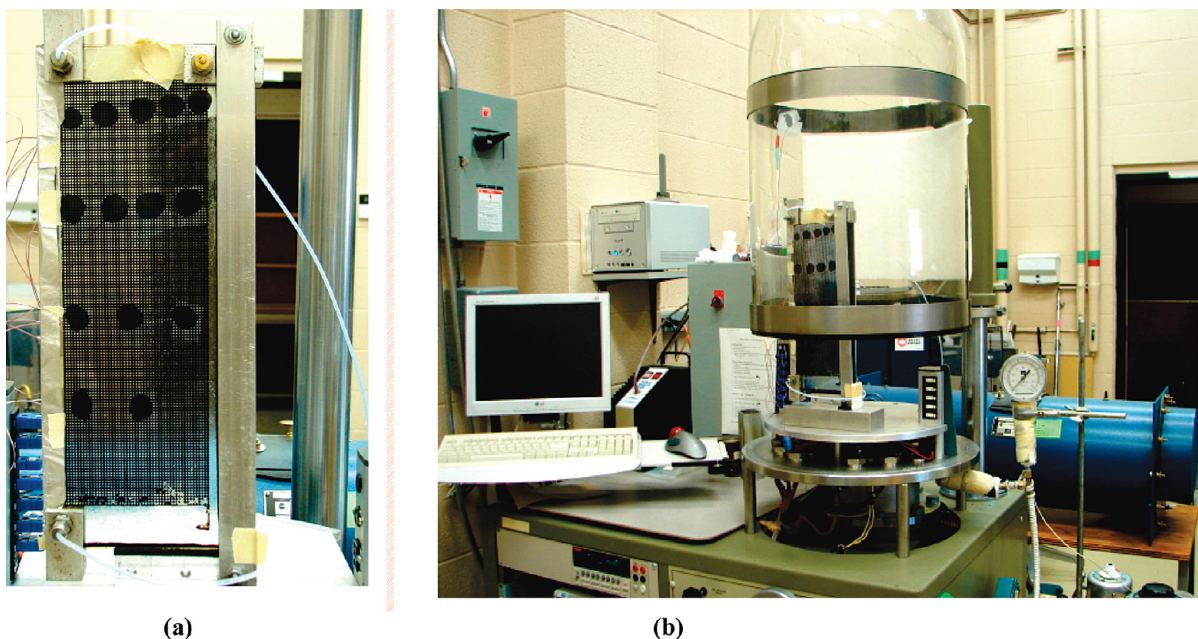


Figure 4. (a) Close-up of glass micromodel saturated with bitumen just before the SA-SAGD visualization experiment. (b) Snapshot of the employed vacuum test rig.

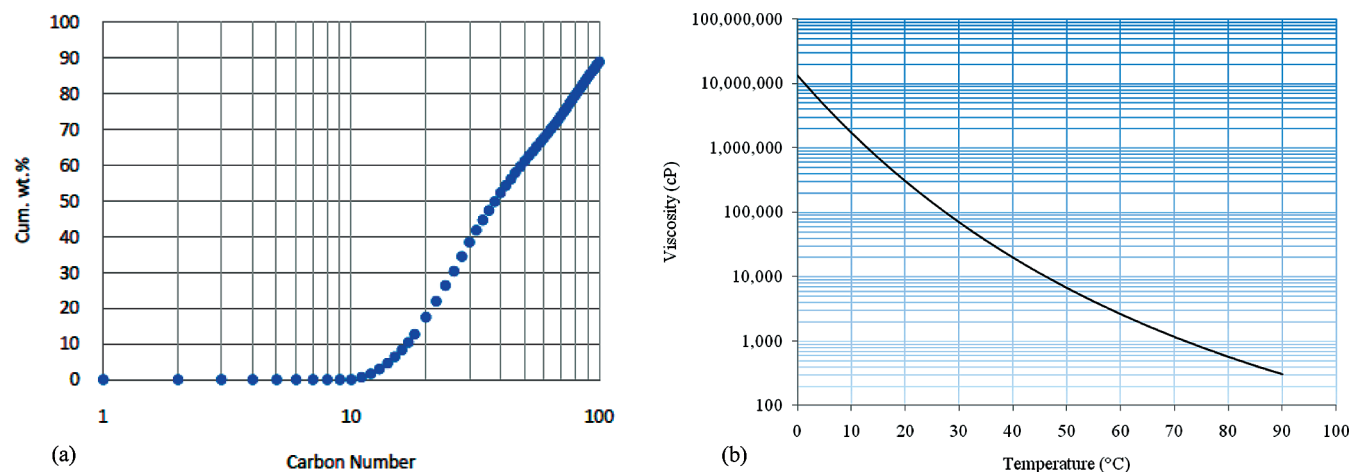


Figure 5. (a) Compositional characteristics of Cold Lake bitumen. (b) Viscosity–temperature relationship of Cold Lake bitumen.

SA-SAGD process at lab conditions suffer from the excessive heat loss from the model to the surrounding environment. As a result of this heat loss, a considerable fraction of the injected steam and its solvent content which are supposed to condense on the cold surface of bitumen, condense in the invaded region of the porous pattern. This condensation process adversely affects the heat and mass transfer processes at the pore-scale and results in condensate phase build-up in the invaded region. As a result, the continuous pathways of the injected vapor toward the interfacial area could be eliminated to the extent that the condensation rate exceeds the drainage rate potential of the model, hence the process could not be continued anymore. In addition, severe condensation of the solvent vapor phase results in extensive asphaltene precipitation once excess liquid solvent is in contact with the in situ bitumen. This phenomenon of asphaltene precipitation, which was experienced in four of our visualization experiments, caused extensive pore-scale clogging of the drainage pathways and prevented the mobilized phases to drain in the direction of flow by gravity.

To facilitate an effective local heating of the bitumen-saturated micromodel in the absence of an undesired heat loss, a vacuum test rig capable of providing up to 10^{-6} Torr of vacuum pressure

was used as an environmental chamber. The vacuum chamber was operated with a combination of a mechanical and a diffusion pump. Figure 4b provides a snapshot of the employed vacuum test rig. All the visualization tests were carried out in the evacuated environmental chamber held at the pressure range of 5×10^{-6} to 10^{-3} Torr. It is believed that at this low air pressure, the amount of heat loss from the glass surface into the surrounding by the convection mechanism is negligible. The only heat loss mechanism that might be of importance at these low magnitudes of vacuum is the radiation heat loss, which could be reduced by covering the hot regions of the micromodel with shiny reflective thin films of materials such as strips of aluminum foil. The heat loss through radiation could also be lowered more by covering some portions of the inverted bell jar glass, which might not be needed from the visibility point of view, with shiny strips of aluminum foil. Operating the SA-SAGD experiments at low values of environmental chamber pressure prevents the vapor phase to condense as a result of undesired excessive heat loss. It also allows the steam and the solvent vapor phases to transfer their latent heat of condensation to the cold bitumen surface where it is intended to be. In other words, the potential of steam and solvent condensation within the vapor chamber is eliminated

Table 2. Range of Operating Conditions for the Performed SA-SAGD Experiments

Vacuum Properties	
vacuum pressure (torr)	5×10^{-6} – 10^{-3}
Steam Properties	
steam temperature (°C)	100–130
steam pressure (psig)	14.7–19.7
<i>n</i> -C ₅ as the Steam Additive	
solvent vapor temperature (°C)	36–75
solvent vapor pressure (psig)	14.7–19.7
solvent content of the steam phase (% vol)	5, 15
<i>n</i> -C ₆ as the Steam Additive	
solvent vapor temperature (°C)	68–95
solvent vapor pressure (psig)	14.7–19.7
solvent content of the steam phase (% vol)	5, 15

Table 3. Employed Fluid Properties

Bitumen	
Density versus Temperature	
bitumen density (g/cm ³)	temperature (°C)
1.012	15
1.001	22
0.997	40
0.978	70
SAPA Analysis	
fraction	mass %
saturates	22.4
aromatics	30.8
polars	29.4
asphaltenes	17.4
Main Elemental Characterization	
element	mass percent
carbon	83.62
hydrogen	9.57
nitrogen	0.39
sulfur	5.25
viscosity at 30 °C	70 000 cP
viscosity at 130 °C	≈1 cP
molecular weight	557 g/mol
Solvent Type 1: <i>n</i> -Pentane	
molecular mass	72.15 g/mol
normal boiling temperature	36 °C
liquid density	0.626 g/cm ³
relative vapor density to air	2.5
Solvent Type 2: <i>n</i> -Hexane	
molecular mass	86.18 g/mol
normal boiling temperature	68 °C
liquid density	0.6548 g/cm ³
relative vapor density to air	3.0

significantly by reducing the heat loss using the vacuum chamber housing for the micromodel.

Figure 5a and b present the compositional characteristics and the viscosity–temperature relationship of Cold Lake bitumen correspondingly. It is worthwhile to note that the normalized weight percent of the heptane plus component (i.e., C₁₀₀⁺) is 10.4 wt % and that of the heavy metals and nonhydrocarbon components is 0.6 wt %. The operating temperature of the conducted SA-SAGD

experiments is dictated by the solvent properties, its associated concentration in the injection main stream, and the volumetric pumping rates of water and solvent. Table 2 contains the range of experimental conditions for the performed SA-SAGD experiments which are categorized according to the type of solvent used in each particular trial. Table 3 presents some general information about the fluid properties in the conducted SA-SAGD experiments.

The observed pore-scale phenomena of the SA-SAGD process during the flow visualization experiments were video recorded. Digital images were also taken at various stages of the process. The images captured from the recorded video were used to document the microscopic events of this recovery technique. Pore-level phenomena on close-up view were captured using a Canon video camera with appropriate combinations of three close-up focusing lenses (+2, +3, and +4). This made it possible to have a particular focused region containing a few pores in view as could be seen in figures presented in this paper. The micromodel was positioned close to one curved side of the inverted bell jar of the vacuum chamber. In order to reduce the reflective problems of the curved glass walls of the chamber and to minimize the parallax, a flat glass or Plexiglas sheet was placed in front of the camera opening to increase the image clarity. The micromodel's surface was divided into cell blocks using a marker to facilitate the frontal position recognition within the porous structure. This makes it feasible to track the interface advancement in terms of the number of pores invaded by the vapor phase. The data collected during each experiment includes, but is not limited to the following:

- (a) Continuous tracking of the vapor–bitumen interfacial position and the average position of the interface within each particular cell block versus experimental runtime (i.e., number of pores invaded versus time).
- (b) Continuous video-recording and digital imaging of the overall shape of the vapor–bitumen interface.
- (c) Continuous video-recording/digital imaging of the pore-scale events.
- (d) Volumetric rate of solvent and steam injection in terms of pumping volume of the cold liquids versus time.
- (e) Continuous real-time monitoring of the glass micromodel's temperature using surface thermocouples at 15 local positions along its surface, and collecting the data using data acquisition system.
- (f) Monitoring the vacuum pressure applied.
- (g) Measuring the final recovery of liquids at each experiment.
- (h) Monitoring the temperature of the injecting phases (i.e., steam and solvent vapor) at the injection side.
- (i) Monitoring the vapor injection line pressure versus time.

Results and Discussion

The pore-scale visualization experiments of the SA-SAGD process at the controlled environmental conditions revealed several heat and mass transfer mechanisms in the vicinity of the apparent gaseous mixture–bitumen interface. As mentioned before, qualitative mass-transfer-related aspects of the SA-SAGD process at the pore-level as well as the microscale flow of different acting phases in the porous structure are described in this paper; however, appropriate referencing to the heat-transport aspects of the process is also delineated whenever it is necessary. Pore-level drainage mechanisms of the mobilized live oil are described as well.

(a) Pore-Scale Event Analysis: Vapor Chamber Early Growth and Its Gradual Outward Development. The presence of a high-permeable trough in the micromodel, extended along one side of the micromodel, provided the means of establishing early communication between the injection and production ports. All of the performed SA-SAGD experiments were initiated with a start-up process in which a steam-only phase was flowing through the high-permeable trough to mobilize the bitumen

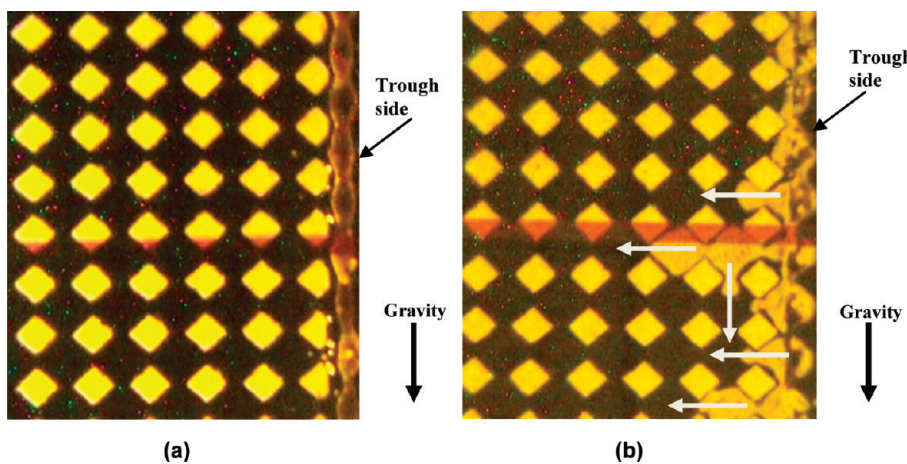


Figure 6. Early lateral propagation of the steam chamber during the start-up stage of the SA-SAGD process (steam-only injection, DL-1 micromodel, steam injection temperature of 110 °C, time interval: 2 min).

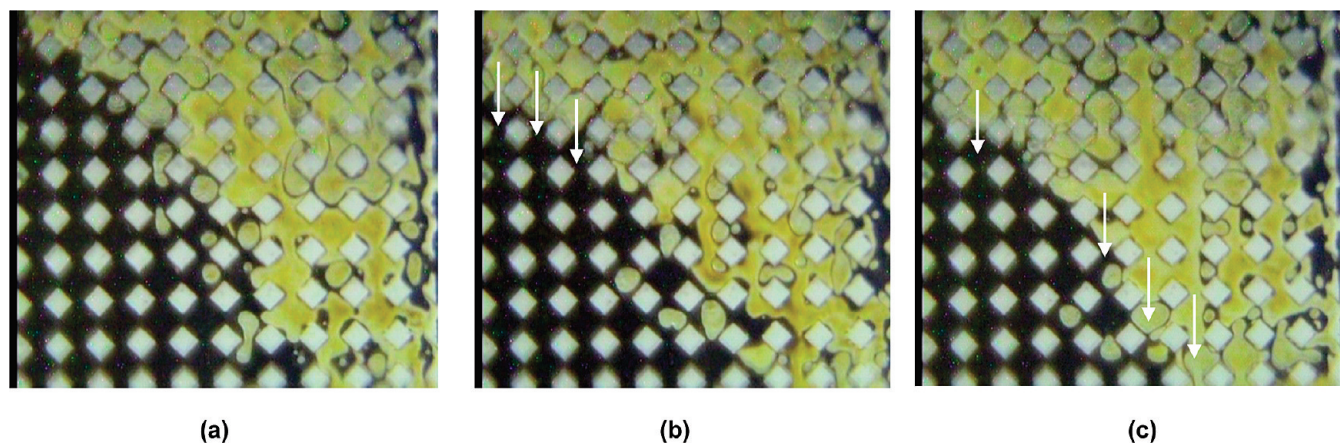


Figure 7. Development stages of the steam/solvent chamber in a typical SA-SAGD process at the pore-scale (OM-1 micromodel, *n*-pentane as the steam additive at 15 vol %, vapor injection temperature of 103.30 °C, time interval: 240 s).

phase present in the neighboring pores of the trough, followed by simultaneous steam and solvent vapor injection. As soon as the bitumen phase achieved enough drainage mobility, the steam phase invaded through the vacated space of these pores, hence the early stages of the vapor chamber growth were initiated. Continuation of this localized invasion of the steam phase through these drained pores is the first sign of the early lateral propagation of the steam chamber, which becomes vapor chamber as soon as the gaseous mixture of steam and solvent is injected instead of the steam-only phase. This pore-level phenomenon, which is supported by the thermal diffusion driving force in the absence of solvent injection during the start-up stage, could be seen in two successive pore-scale snapshots shown in Figure 6. Mobilized oil drained out of these pores and steam invaded through them following the sequential behavior of drainage type displacement in a pore mechanism during an immiscible displacement process.³³

Similar to the case of the SAGD chamber development, the steam/solvent chamber in the SA-SAGD process at the pore-level could be defined by the continuum of the gas-invaded pores, which is dendritic in nature during the early development stages of the chamber. These invaded pores by the vapor are well-interconnected from the gas flow point of

view; however, there is possibility of condensation at the tip of each contact point of the gas-invaded pores with the bitumen-filled pores. The local condensation of vapor could happen either in a pore constriction or within the entire pore body, resulting in creation of water condensate droplets or those of the liquid solvent. Figure 7 shows the evolution stages of the SA-SAGD vapor chamber when both solvent and steam phases are injected through the injection main stream. One can clearly observe the state of fluid distribution as well as condensation phenomenon at the pore-scale through these subsequent snapshots. One can find several vertically and horizontally oriented pore constrictions which are filled either with the bypassed oil, or with the trapped nonwetting droplets of condensate, ahead of the interfacial region toward the invaded pores. The presence of these flow barriers deteriorates the gaseous phase flow toward the interfacial region and, hence, demotes the rate of the microscale mass transfer process.

One can realize the different flow zones presented in the vicinity of the apparent SA-SAGD interface based on our flow visualization results. In the case of the noncondensing SA-SAGD process, the pores adjacent to the apparent interface drain preferentially in the direction of gravity and form dead-end type of structures. As a result, the drainage of oil films could then be redirected, which leads to creation of a peaks-and-valleys configuration of the flow pathways at the

(33) Chatzis, I.; Dullien, F. A. L. *J. Colloid Interface Sci.* **1983**, 91 (1), 199–222.

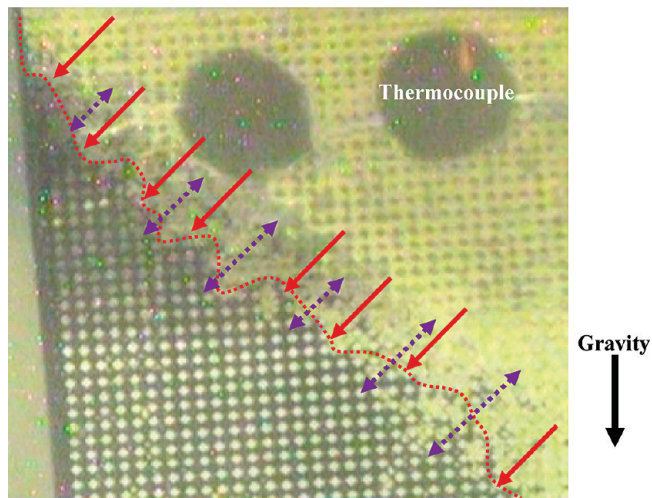


Figure 8. Visualization of the skeleton of the noncondensing SA-SAGD interface, flow pathways of the gaseous phase, and the mobilized region (OM-2 micromodel, *n*-hexane as the steam additive at 5 vol %, vapor injection temperature 110.60 °C, time 9050 s).

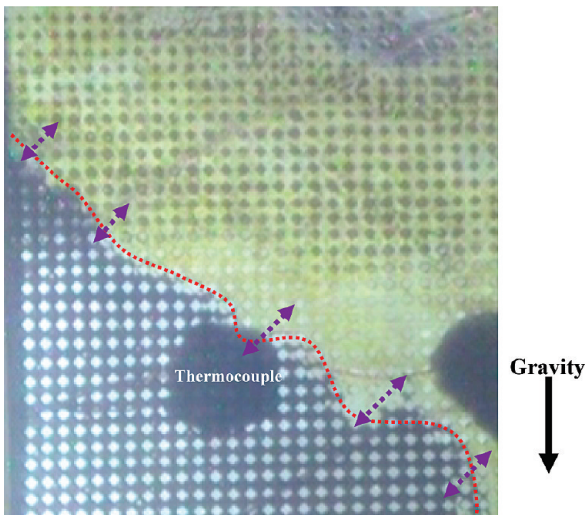


Figure 9. Visualization of the skeleton of the condensing SA-SAGD interface, flow pathways of the gaseous phase, and the mobilized region (OM-2 micromodel, *n*-hexane as the steam additive at 15 vol %, vapor injection temperature 101.85 °C, time 7055 s).

nominal interface such as those pointed out with dark red arrows in Figure 8. The presence of a peaks-and-valleys type of interfacial pattern, which is presented by the fine-dotted tortuous red curve in Figure 8, could be avoided if continuous films of the mobilized live oil exist at the pore scale, as this is the case in the condensing mode of the SA-SAGD process (Figure 9). These finite-in-length continuous films of the mobilized live oil flow down gradient just ahead of the apparent SA-SAGD interface and fill the localized valleys to the extent of creating a relatively smooth apparent interface, extended vertically under the action of gravity. This is shown by the fine-dotted smooth red curve in Figure 9. No matter the form of the apparent SA-SAGD interface, it is located just behind a layer of pores composed of 1–5 pores in thickness which is the so-called “mobilized region”.

(b) **Qualitative Pore-Scale Event Analysis within the Mobilized Region.** The combined effects of thermal mobilization

drive as well as solvent diffusion and convection create a region, so-called mobilized region, in which different interacting fluid phases are flowing simultaneously. This region contains different fluid phases including:

- Gaseous phase: A mixture of the steam and the solvent vapor, in the form of channeled finite-pores-extended bubbles of the gaseous phase, flow through this region in a convective manner.
- Liquefied phases: These phases include the condensed steam as the main liquid phase and the condensed solvent phase. The condensed solvent could be either in the form of localized liquid solvent in water emulsion phase (i.e., water as the continuous phase and liquid solvent droplets as the dispersed phase based on the volumetric contrast of the liquids), or in the form of small liquid solvent droplets or even in the form of finite-pores-extended films of liquid solvent diluting the bitumen phase.
- Mobilized live oil: The presence of this liquid phase depends on the viscosity-reduction process of the bitumen under the simultaneous heat and mass transfer phenomena at the pore-level. This liquid phase drains in the form of thin finite-pores-extended films of the mobilized live oil over the bitumen-saturated pores under the action of gravity.

The draining phases (i.e., the mobilized live oil as well as the steam and solvent condensate phases) are flowing downward parallel to the nominal SA-SAGD interface. Our visualization experiments revealed that the thickness of the mobilized region varies at different particular elevations and is in the order of 1–5 pores in depth ahead of the nominal SA-SAGD interface. In this region, whose thickness is shown by dotted purple arrows in Figures 8 and 9, most of the convective nature of the SA-SAGD process is observed in the form of severe pore-scale local mixing in the vicinity of the apparent interface. The average thickness of the mobilized region along the entire drainage head depends on several parameters such as operating conditions (i.e., temperature and pressure) as well as the solvent type. Most of the transport processes at the pore-level, such as microscale diffusion and convection mass transfer as well as microscale heat transfer in the form of conduction and localized convection take place within the thickness of this region. Different acting forces are contributing to the simultaneous fluid flow within this region, namely gravity, capillary, and buoyancy forces in the absence of excessive viscous force. This mobilized region is mainly formed due to the presence of thermal diffusion at the pore scale, and it clearly has an oriented structure, in which different draining fluid phases are flowing parallel to the nominal SA-SAGD interface. Unlike the limited drainage depth of the mobilized live oil in the VAPEX process, which is in the order of 1–2 pores,^{26,34} our visualization results revealed that the depth of SA-SAGD mobilized region (δ_m) is at least 2 times thicker compared to that of the VAPEX process. This is due to the higher magnitude of the thermal diffusion and convection as a measure of the extent of the heat transfer process, as well as the supplementary contribution of the solvent dilution phenomenon at the SA-SAGD process compared to that of the molecular diffusion only, which is responsible for the local mass transfer aspects of the region".

(34) James, L. A.; Rezaei, N.; Chatzis, I. VAPEX, Warm VAPEX, and Hybrid WAPEX - The state of enhanced oil recovery for in-situ heavy oils in Canada. *J. Can. Pet. Tech.* April 1–7, 2008.

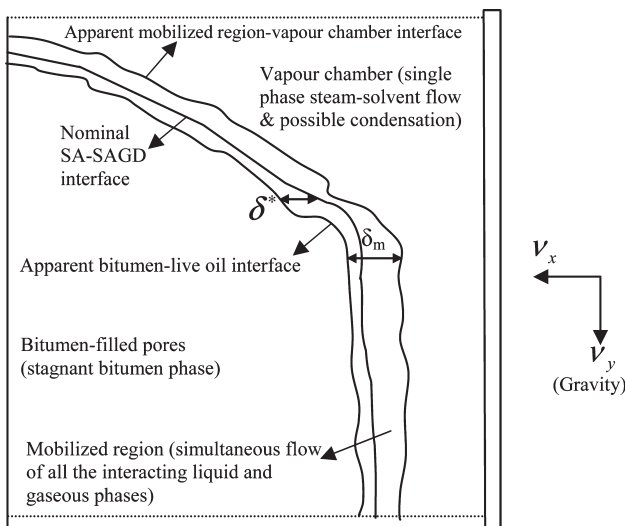


Figure 10. Schematic pore-level diagram of fluid flow zones in a typical SA-SAGD process based on the qualitative flow visualization results.

conventional VAPEX process. This point could also be verified knowing the fact that the oil within the pores behind the SA-SAGD nominal interface, in a distance composed of 1–4 pore body widths, is also being mobilized as a combined effect of localized heat and mass transfer. As it is evident in Figure 7, both the entrapped droplets of the condensate and the enclosed bubbles of the gas phase drain within the oil continuum right behind the nominal SA-SAGD interface.

Transport mechanisms involved in a SA-SAGD process include heat transfer by thermal diffusion and convection, mass transfer by molecular diffusion and convection, convective mixing of the gaseous phases and the liquefied phases with the mobilized heavy oil, and the gravity drainage of the viscosity-reduced oil along with the water condensate and the liquefied solvent. The mobilized live oil and also the liquefied phases drain within the mobilized region by the action of gravity force when it overcomes the capillary and possible viscous forces. The predominant factor for the drainage of bitumen is the reduction of viscous drag due to the exponential reduction of the bitumen in situ viscosity upon the combinatory effect of steam heating and solvent dilution. The role of gravity force and capillary force depends on the individual drainage mechanisms at the pore-scale. According to our flow visualization experiments, there are different pore-level fluid flow zones in a typical SA-SAGD process which are schematically presented in Figure 10. These flow zones were characterized according to the type and thermodynamic state of the fluids flowing in each particular region as follows:

- Vapor chamber in which the injected gaseous phases are the predominant flowing phases. There is possibility of condensation through this region, followed by condensate drainage in the direction of gravity.
- Bitumen-filled pores: This zone is the stagnant zone in which in situ bitumen viscosity is still beyond the mobilization limit. The exact external boundaries of this zone could not be easily recognized when a film of the mobilized live oil is draining over it. Heat is transferred to this zone across the apparent bitumen–mobilized live oil interface by a combination of conduction and convection mechanisms. Engulfed-in-oil droplets of hot water

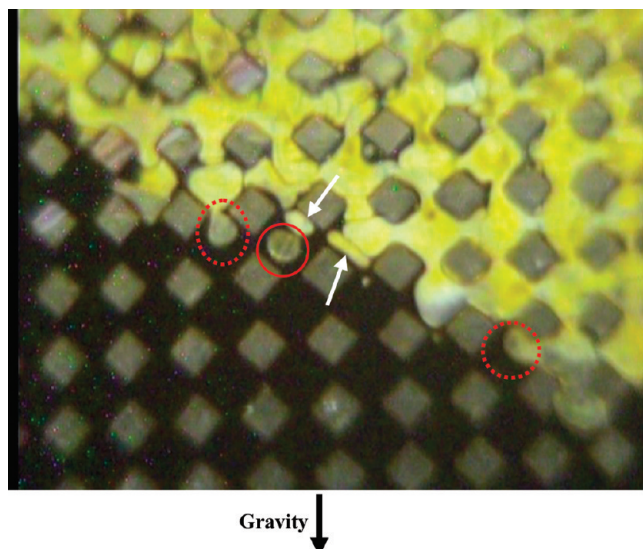


Figure 11. Vapor chamber in direct contact with the oil continuum at the pore-level (DL-1 micromodel, *n*-pentane as the steam additive at 5 vol %, vapor injection temperature of 102.50 °C, time 6620 s).

condensate as well as isolated bubbles of the vapor phase are responsible for the convective element of the heat transfer at the pore-scale. Mass transfer also occurs in this zone to a limited depth by the diffusion mechanism.

- Mobilized region, whose thickness is expressed as $\delta_m|_{\text{SA-SAGD}}$ in Figure 10, is the region in which simultaneous flow of all the acting fluid phases is observed.
- Mobilized live oil film, whose thickness is expressed as $\delta^*|_{\text{SA-SAGD}}$ in Figure 10, is a subdivision of the mobilized region in which thin layers of the mobilized live oil film are draining over the bitumen-filled pores. As soon as this liquid region attains appreciable thickness (i.e., in the order of 1–2 pores) as a result of the miscibility nature of the SA-SAGD process over time, some small droplets of the condensed steam and solvent as well as small gaseous bubbles could be enclosed within the thickness of this region and then be dragged and drained along with the mobilized live oil film in the direction of gravity.

The above-mentioned fluid flow zones are separated from each other with hypothetical distinction lines (or distinction surfaces when the 3D skeleton of the pore structure is concerned) according to the schematic diagram presented in Figure 10, namely:

- Apparent mobilized region–vapor chamber interface: This is a demarcation line (or demarcation surface) between the vapor invaded pores and the pores within the mobilized region at the microscopic scale.
- Nominal SA-SAGD interface: This is a distinction line (or distinction surface) between the pores in which the live oil phase is draining as a film over the bitumen-saturated pores and the pores in which all the interacting phases are draining simultaneously (i.e., mobilized region). In other words, this microscopic interface is defined between the mobilized region and the thin mobilized live oil film.
- Apparent bitumen–live oil interface: This demarcation line is defined as the pore-level interface separating the bitumen-saturated pores and the pores in which the live oil is flowing as thin films although it is difficult to distinguish between these two regions even at the magnified pore-level

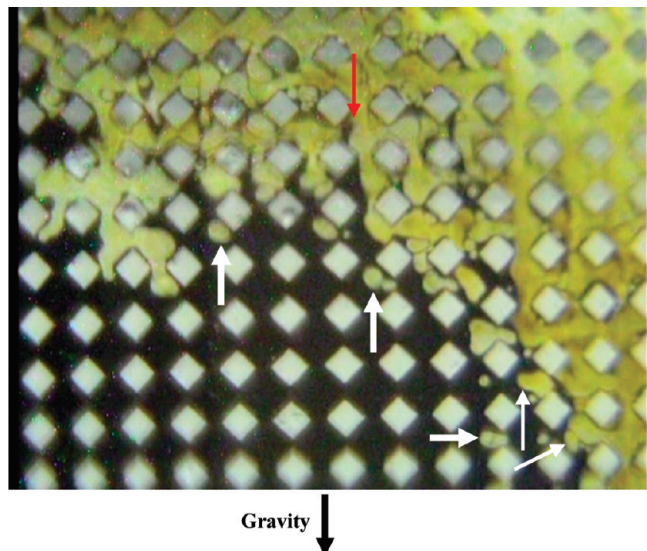


Figure 12. Closer look at the pore-level mobilized region of the SA-SAGD process (DL-1 micromodel, *n*-hexane as the steam additive at 5 vol %, vapor injection temperature of 108.30 °C, time 6050 s).

snapshots. The extent of the mobilized live oil film flow over the bitumen-saturated pores could cause periodic thickening and thinning of the oil wedge which could be recognized through the pore-scale snapshots and the recorded video.

The term “live oil” could be assigned to that oil phase at the pore-level in which one can find a finite concentration of solvent. Part of this live oil could drain as its viscosity is reduced to the extent of its mobilization under the action of gravity, which is named “mobilized live oil” film, whose thickness was defined as $\delta^*|_{\text{SA-SAGD}}$. Figures 11 and 12 present a closer look at the mobilized region at the pore-level. Figure 11 shows the contact of the gaseous phase with the oil phase just at the nominal SA-SAGD interface, i.e. all the pore bodies below this particular location contain only oil phase. One can see the condensation phenomenon at the tip of the invading gaseous phase, as well as the bypassed oil within some pore throat constrictions. Some of the bypassed oil drains in the form of film flow in the corners of the pores which were already invaded by the gaseous phase. In addition, droplets of condensate ahead of the invading gaseous phase are engulfed within the down-structured continuum of the oil phase as is indicated by solid red circle in Figure 11. The dotted red ellipses show the locations where an isolated droplet of condensate is being formed due to the snap-off mechanism. Tiny bubbles of the gaseous phase could also be encapsulated by the down-structure continuum of the mobilized live oil as are depicted by white arrows in Figure 11. Figure 12 shows a closer look at the extended mobilized region of the SA-SAGD process. Red arrow shows the vertically oriented film flow drainage of the mobilized live oil in the presence of the gaseous phase. One can clearly note the distribution of all three flowing phases within this pore-scale snapshot. In Figure 12, all the aforementioned flow zones of a typical SA-SAGD process at the pore-level could be observed such as the mobilized region followed by the gas-invaded pores to the top right of the figure, apparent SA-SAGD interface, and the oil-saturated pore bodies behind the nominal interface to the bottom left of the figure. It is clear that some small bubbles of the gaseous phase were trapped within

the draining live oil (i.e., beneath the interface to the left), which are pointed out by thin white arrows. In addition, enclosure of small droplets of condensate is also evident within the continuum of the mobile oil just behind the nominal interface (i.e., thick white arrows). Continuous drainage of these trapped bubbles and droplets is an evidence that the oil phase behind the nominal SA-SAGD interface within a limited distance in the order of 1–4 pore body widths is mobile enough to drain in the direction of gravity.

(c) Pore-Scale Drainage Mechanisms. According to the flow visualization results, two drainage mechanisms were found responsible for the pore-scale recovery of a typical SA-SAGD process, namely the (1) capillary drainage displacement mechanism and (2) film-flow drainage mechanism. These two simultaneous mechanisms are responsible for displacing the already-mobilized-oil with the aid of gravity and capillary forces within the mobilized region and the invaded area, and also through a limited distance behind the SA-SAGD nominal interface.

(c.1) Capillary Drainage Displacement Mechanism. This drainage displacement mechanism is responsible for most oil recovery during the SA-SAGD process at the pore-level. Under this displacement mechanism, a finite-pores-extended volume of the mobilized oil drains within the mobilized region and even behind it through a limited distance of about 1–4 pore bodies by direct drainage of oil from the oil-filled pores by the invading gaseous phase according to the typical sequential drainage displacement of a wetting phase using a nonwetting phase at the pore scale.³³ This direct drainage displacement is facilitated with the aid of gravitational force in the absence of excessive viscous forces. This direct invasion of the gaseous phase through the pores which are already filled with the mobilized oil creates extensive local mixing within the mobilized region just ahead of the apparent SA-SAGD interface at the pore-level. Our visualization experiments revealed the existence of severe local mixing within the mobilized region. This type of displacement is indicated by white arrows in Figure 6. In addition, Figure 7 provides a series of pore-scale events including sequential drainage displacement of the wetting phase by the invading gaseous nonwetting phase in the direction of the white arrows over a four-minute time period. As the oil in contact with the gaseous phase is already heated to the extent of being readily mobile, it is convenient to observe direct drainage of several pores in a serial format simultaneously within the interfacial region. This drainage mechanism is also presented in Figure 13 through five subsequent pore-level displacement images.

As is depicted in Figure 13, the gaseous mixture of steam and *n*-hexane vapor displaces the already mobilized oil in the direction of thick white arrows. The invading nonwetting phase front is pinched-off in some pores by the capillary phenomenon of the snap-off mechanism while displacing the wetting phase (i.e., live oil) under the direct capillary drainage displacement mechanism. This snap-off phenomenon is due to the unstable nature of the advancing nonwetting phase front as well as capillary instabilities caused by the local pore structure. As a result, small bubbles of the gas phase were enclosed within the draining column of the mobilized oil. In Figure 13, these isolated bubbles of the gaseous phase and engulfed droplets of the condensate are shown by red and yellow arrows, respectively. These enclosed phases drain downward along with the live oil ahead of the invading front of the nonwetting phase. These frequently occurring pore-scale events enhance the extent of both the mass and heat transfer processes. The isolated gas bubbles can reconnect to the bulk of the gaseous phase (i.e.,

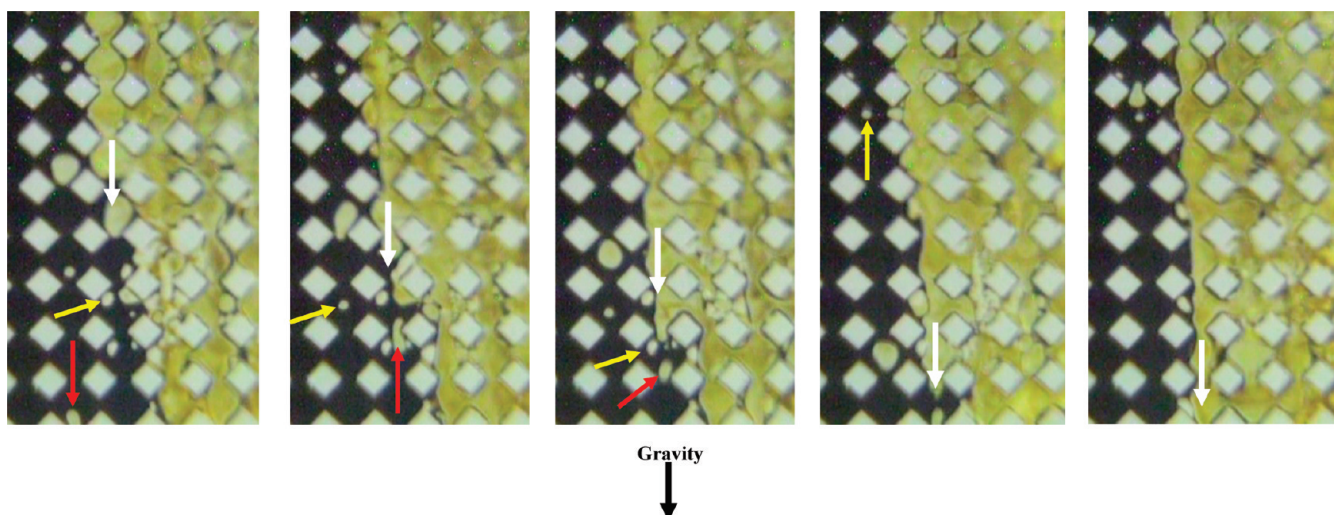


Figure 13. Sequential drainage of the wetting phase by unstable invading front of the nonwetting gaseous phase under the direct capillary drainage displacement mechanism at the pore-level (DL-1 micromodel, *n*-hexane as the steam additive at 5 vol %, vapor injection temperature of 109.70 °C, time interval 180 s).

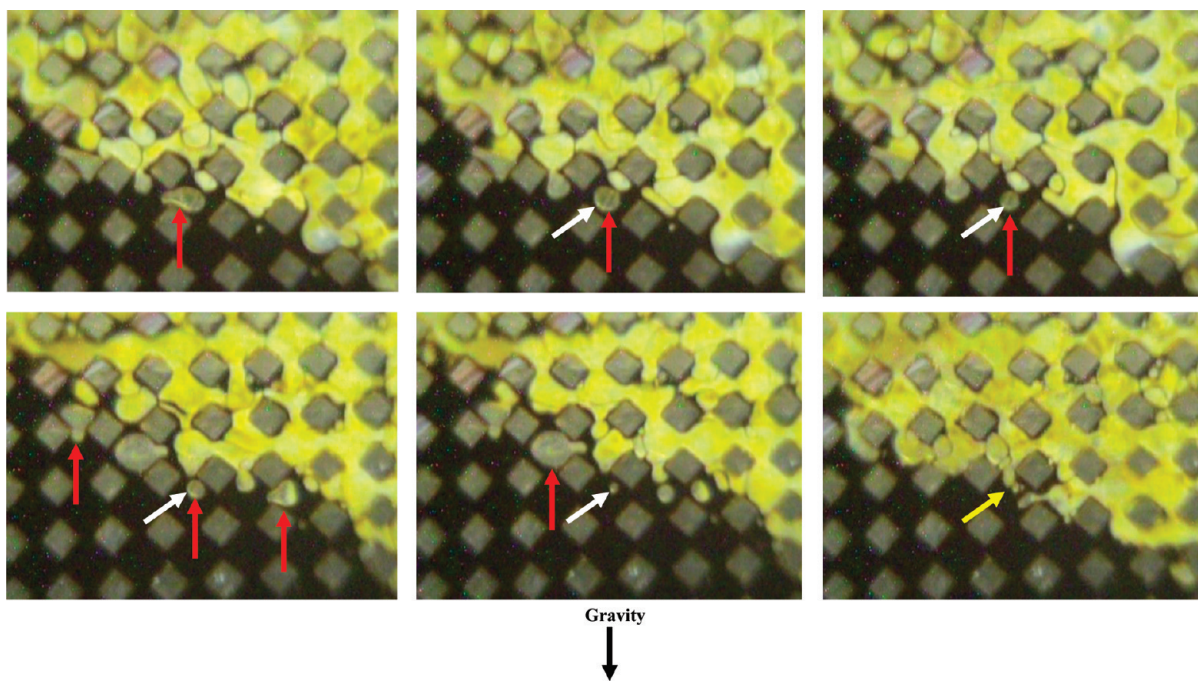


Figure 14. Snap-off mechanism occurred at the unstable invading front of the displacing liquid phase, followed by droplet shrinkage phenomenon at the pore-scale due to the local mass transfer process (DL-1 micromodel, *n*-pentane as the steam additive at 5 vol %, vapor injection temperature of 104.05 °C, time interval 320 s).

vapor chamber) if they maintain their gaseous state at the time of gas invasion into a pore containing live oil and a gas bubble. Aside from this reconnection scenario, these isolated gaseous bubbles could also condense while moving down gradient due to the excessive heat loss. An excessive volume shrinkage phenomenon due to the phase change was also observed, which is an indication of the localized heat transfer process at the pore-scale.

If a solvent condensate droplet is enclosed within the continuum of the mobilized oil, its volume shrinks as a result of the local mass transfer at the pore-level. The enclosed solvent condensate droplet disappears over time because of the solvent diffusion into the oil if an extended-enough drainage path is available within the live oil continuum. On the other hand, if a water condensate droplet is engulfed within the live oil phase, it

could propagate within the oil continuum in the form of a dispersed water phase in oil, composing the in situ water in oil emulsion at the pore-scale. Figure 14 shows a series of events starting from the encapsulation process of the snapped-off liquid droplet at the pore-level (i.e., red arrow), followed by local mass transfer processes which cause the shrinkage of the enclosed droplet at static conditions where the droplet is stagnant within the pore body (i.e., white arrow). Finally, a coalescence stage exists for some droplets when the contracted condensate droplet is reconnected to the invading liquid front (i.e., yellow arrow).

(c.2) *Film-Flow Drainage Displacement Mechanism.* The mobilized and bypassed oil could also drain as a result of film-flow drainage in the corners of pore space that were invaded by the gas phase. The extent of film flow drainage is

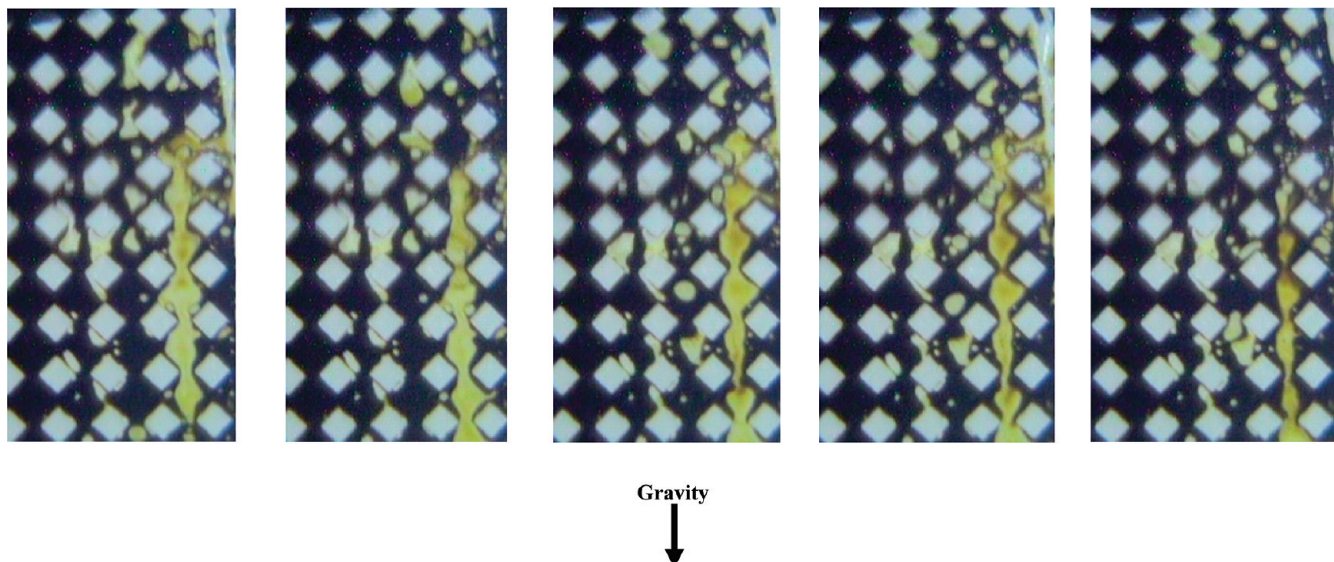


Figure 15. Film-flow drainage of the mobilized live oil at the pore-scale during a time span of 52 s (OM-2 micromodel, *n*-hexane as the steam additive at 5 vol %, vapor injection temperature 108.90 °C).

much more pronounced in a three-dimensional porous medium compared to that in a simple 2D porous structure due to pore interconnectivity and dimensionality. In a typical SA-SAGD process, this type of drainage mechanism happens in the vicinity of the nominal SA-SAGD interface (i.e., within the mobilized region as well as inside the invaded zone). Periodic formation and rupture of the finite-in-length live oil films within the mobilized region, due to the convective nature of the drainage process at the pore-scale within this region, limits the extent of film flow drainage within this zone. However, one can observe the frequent thickening and thinning of the mobilized live oil film in the corners of the gas-filled pores ahead of the nominal SA-SAGD interface. These draining live oil films could alternatively fill some down-structured pore bodies or pore throats and, as a result, would smooth off the nominal SA-SAGD interface in the form of a vertically extended type of interface. According to the pore-scale observations, momentum transfer at the pore-level does not happen only in one vertical column of pores. Although the nominal SA-SAGD interface at the macroscale looks like a continuous distinctive line (or surface) between the bitumen-filled pores and the swept region filled with the vapor phase, it contains numerous irregularities at the microscale in the form of a peaks-and-valleys-type of interfacial structure. However, due to the film flow of the live oil over the nominal SA-SAGD interface and the miscibility conditions in this process compared to that of the SAGD, the extent of tortuousness in the interface is much less in the SA-SAGD compared to that in the SAGD.

However, one could still observe some oil-filled pores protruding irregularly into the vapor-filled pores of the swept region of the SA-SAGD process. It is clear that these oil-filled pores contain mobilized live oil draining down gradient mainly by the capillary drainage displacement mechanism.

As a result of the film-flow drainage of mobilized live oil in pores invaded by gas and also through the vertically oriented mobilized-live-oil-filled pore constrictions, the apparent interface between the vapor and the mobilized live oil would be repositioned from the junction of the mobilized-live-oil-filled pore throats and vapor-filled pore bodies to the vertical

midway within the pore bodies which were filled previously with the vapor phase. This frequent repositioning of the interfacial location, which shows in the form of repeated thickening and thinning of the interfacial layer, is evidence of the presence of extensive film-flow drainage. The pore-scale events of the nonwetting phase bubble and droplet formation within the oil continuum during the direct invasion of a pore filled with the mobilized live oil by the invading gas phase was described in section c.1 where the relevant sequence of pore-level events was analyzed. The same sequence of events is also observed during the film-flow drainage mechanism at the pore-level. A finite bubble of the vapor phase occupying one to several pores or a droplet of the liquefied phase could be truncated as a result of the film-flow of the mobilized live oil in the corners of a particular pore, or a series of pores, containing the nonwetting phase. This truncated nonwetting phase is isolated within the surrounding oil phase whose main source is the drained films of oil. Subsequently, the entrapped nonwetting phase undergoes through the shrinkage/disappearance process at the pore-level either in a static or in a dynamic situation. In other words, this trapped nonwetting phase may (a) remain stationary if the drainage velocity of the surrounding mobilized oil does not overcome the buoyancy forces applied if it is vapor or (b) flow downward along with the surrounding mobilized live oil. In either of these two cases, the shrinkage/disappearance process happens due to the heat and mass transfer processes at the pore-level. There is also the possibility of reconnection/coalescence of each particular entrapped nonwetting phase either with the continuum of the vapor phase in case if it is an isolated vapor bubble or with the other enclosed droplets of the liquefied phases in case it is an isolated liquid droplet. In Figure 12, the downward facing red arrow shows limited extent of film flow within the mobilized region. In addition, Figure 15 shows the extent of film-flow of the live oil in the corners of gas-filled pores which leads to pore-refilling by the wetting oil phase.

As far as the swept region is concerned, the oil films left behind could periodically form loop structures involving finite films within the continuum of the gaseous phase. If these films keep their inherent flow continuity over the limited distance of their extension, there is possibility of oil drainage under film flow

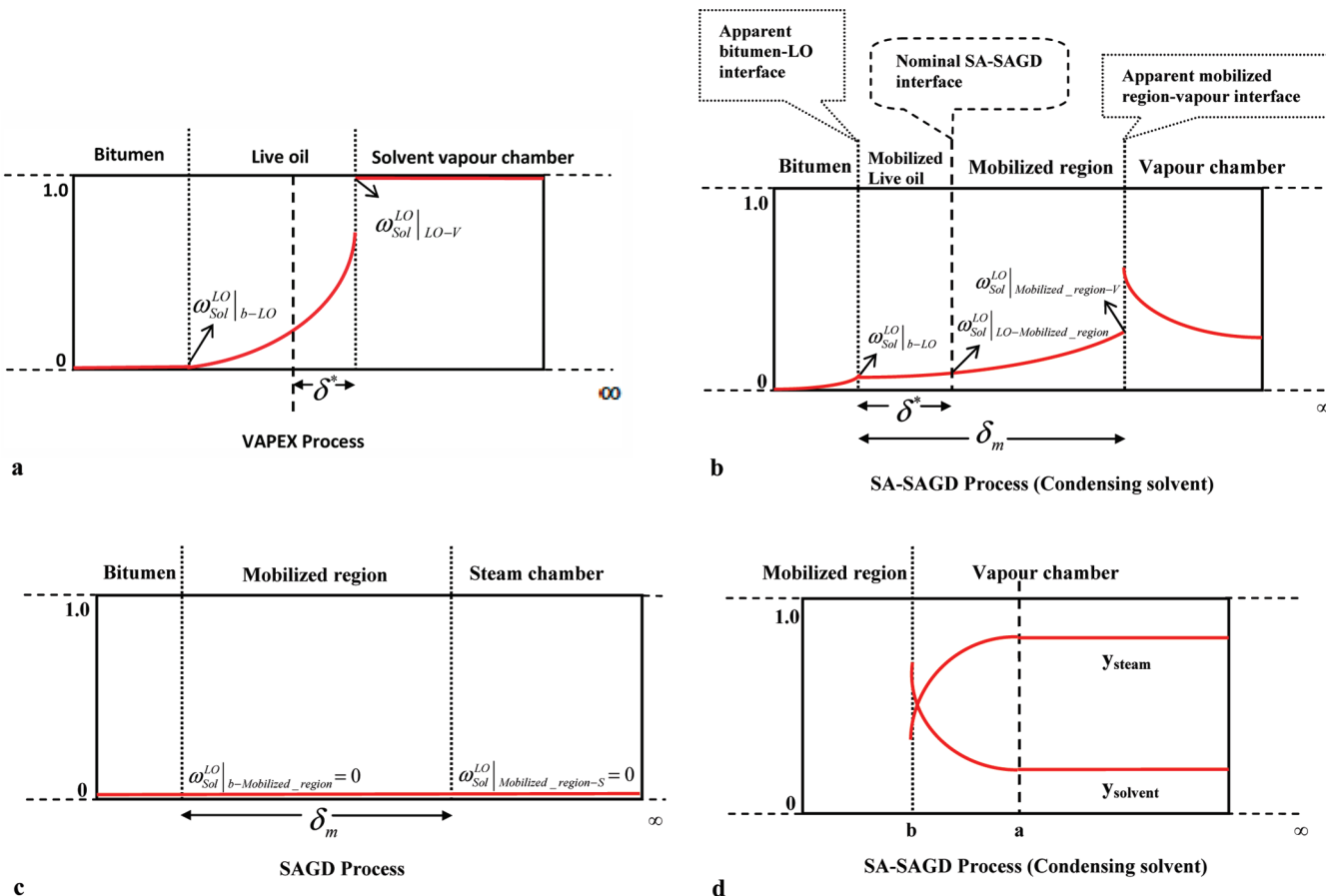


Figure 16. (a–c) Schematic solvent concentration profile across the cross-sectional area of the VAPEX, SA-SAGD, and SAGD processes, respectively. (d) Schematic diagram of solvent vapor and steam mole fraction gradients across the cross-sectional area of the SA-SAGD process.

drainage mechanism within the invaded area. The drainage rate of these closed-loop oil films is lower than that of the bulk oil within the pores when displaced by the direct invasion of gas. However, high degrees of local mixing associated with the invaded area and the mobilized region as well as the miscible nature of the SA-SAGD process lower the residual oil saturation within the vapor chamber. These two factors usually do not allow sufficient flow continuity for the draining oil films ahead of the nominal SA-SAGD interface. When these oil films attain enough continuity over their extension within the invaded area, they are capable of creating some finite-pores-extended regions of mobilized live oil within the swept region. The existence of these regions of live oil within the vapor chamber depends on the extent of the live oil film flow in the corners of the pores already filled with the vapor phase. The pore-scale mobilization process of these finite and mobile live oil regions that appear to be bypassed takes place through a combination of drainage and imbibition processes. The downward moving front-end of these mobile live oil regions advance down gradient by the imbibition process and displace the vapor-filled pores ahead, while the trailing-ends of these structures undergo displacements by the drainage mechanism.

(d) Mass Transfer Mechanisms at the Pore-Scale. For a typical SA-SAGD process, the dominant pore-scale mobilization mechanism is due to oil viscosity reduction by heat transfer and gravity drainage. Visualization studies of the SA-SAGD process reveal that there are complex interactions between all the flowing phases draining by gravity at the interfacial region. Mass transfer of the solvent phase into the live oil could take place by molecular diffusion, hydrody-

namic mixing caused by capillary phenomena, and convection. It is evident that because of the convective nature of the process, especially within the mobilized region in which there is pore-level convective mixing, the role of the convective mass transfer is greater than that of the molecular diffusion. However, diffusion mass transfer still occurs along the drainage pathways of the flowing oil phase. It is evident that the mass transfer mechanism in a solvent-aided heavy oil recovery process significantly depends on the thermodynamic state at which the solvent phase is in contact with the bitumen. For instance, if the solvent condenses at the bitumen interface, the convection mass transfer from bitumen to the liquid solvent will significantly enhance the process of oil extraction. Depending on the “condensing” or “noncondensing” state of the solvent in contact with the bitumen, different mass transfer mechanisms seem to be more important.³⁶ It is believed that the overall performance of the SA-SAGD process would be optimized only if the solvent condenses within the mobilized region ahead of the nominal SA-SAGD interface. In a solvent aided recovery process, it is generally accepted that the mass transfer process could be conducted by diffusion and convection of the solvent present in the injected vapor phase as it transfers into the heavy oil and vice versa, based on the pore-scale concentration gradient

(35) Firoozabadi, A. *Thermodynamics of Hydrocarbon Reservoirs*; McGraw-Hill, New York, 1999, ISBN-13: 978–0070220713.

(36) Rezaei, N.; Mohammadzadeh, O.; and Chatzis, I. *Improving the Performance of Vapour Extraction of Heavy Oil and Bitumen using the Warm VAPEX Process*. Proceeding Canadian Unconventional Resources and International Petroleum Conference 2010, SPE 137824, Calgary, Alberta, October 19–21. (DOI: 10.2118/137824-MS).

present at the interfacial region. There is a dramatic decline in the magnitude of in situ viscosity of the bitumen phase due to the combined effect of heat and mass transfer. Each of these two transport processes could profoundly reduce the bitumen viscosity. As a result, the synergistic effects of convective/capillary mixing and heat and mass transfer enhance the volumetric sweep efficiency of the SA-SAGD process at the pore-scale.

(d.1) *Microscopic Solvent Concentration Gradient.* As the solvent chemical potential gradient across the interfacial region is the main driving force for the pore-level interfacial mass transfer in a solvent aided process of heavy oil recovery, it is important to analyze it for different typical recovery schemes. Here, three main in situ bitumen recovery processes are schematically characterized based on different flow zones present near the interfacial area of each particular process. Figure 16a–c schematically shows the solvent concentration profile across the interfacial area of three main processes of VAPEX, SA-SAGD, and SAGD, respectively. According to Figure 16a, the solvent concentration within the solvent chamber is 100% for the VAPEX process if the injected solvent is pure. There is a dramatic decline in the solvent concentration of the live oil at the live oil–solvent vapor interface ($\omega_{\text{Sol}}^{\text{LO}}|_{\text{LO}-\text{v}}$) to that of the live oil at the bitumen–live oil interface ($\omega_{\text{Sol}}^{\text{LO}}|_{\text{b}-\text{LO}}$). The former depends on the vapor–liquid equilibria (VLE) of solvent/live oil pair and the k -factor which relates the proportion of the solvent mole fraction in the vapor phase to the liquid phase solvent mole fraction in the live oil film at the interface, while the latter is close to zero at the stagnant bitumen face. In the VAPEX process, the maximum pressure applied through the invaded region in the absence of either steam or an inert gas is the vapor pressure of solvent that corresponds to the operating temperature. The VAPEX process could be categorized into condensing and noncondensing modes depending on the operating pressure and temperature which dictate the thermodynamic state of the solvent phase near the nominal VAPEX interface. In this figure, the thickness of the mobilized live oil film draining over the bitumen-saturated pores is shown by δ^* .

Figure 16b shows the schematic diagram of the solvent concentration in a typical SA-SAGD process. In such a process, the solvent concentration in the invaded area is limited to low values of solvent being injected along with the steam phase. As is shown in this diagram, there is a solvent concentration gradient within the invaded portion of the porous medium from its predetermined value at the injection side to the solvent mole fraction in the vapor phase at the interface between the mobilized region and the vapor chamber. There is also a temperature gradient within the invaded area of a typical SA-SAGD process even if the steam–solvent gaseous mixture is injected continuously. As a result of this temperature gradient, steam is the first component to condense even before reaching the interfacial area between the mobilized region and the gas-saturated pores. As a result, the steam concentration of the injected vapor experiences a gradual decline within the vapor chamber. On the other hand, solvent concentration in the vapor phase increases significantly near the mobilized region–vapor chamber interface as it is the last component in the vapor phase to condense based on the temperature gradient present within the vapor chamber. Depending on the vapor–liquid equilibria of the solvent–steam–oil system at the apparent interface between the mobilized region and the vapor chamber, the solvent content at the interface of the live oil varies from the solvent content of the vapor phase at this interfacial region. There is a decline in the magnitude of the live oil solvent

content from its value at the apparent mobilized region–vapor chamber interface (i.e., $\omega_{\text{Sol}}^{\text{LO}}|_{\text{mobilized_region-v}}$) to its value at the apparent mobilized live oil film–mobilized region interface (i.e., $\omega_{\text{Sol}}^{\text{LO}}|_{\text{LO-mobilized_region}}$). This decline in the solvent content value in the live oil is continued, from its magnitude at the apparent mobilized live oil film–mobilized region interface ($\omega_{\text{Sol}}^{\text{LO}}|_{\text{LO-mobilized_region}}$) to its value at the bitumen–mobilized live oil film ($\omega_{\text{Sol}}^{\text{LO}}|_{\text{b-LO}}$) where the bitumen phase still contains some limited solvent content to the extent at which it could no longer be considered as the “raw bitumen”. The finite magnitude of the solvent content of the bitumen phase at the apparent bitumen–mobilized live oil film interface causes another decline rate in the solvent concentration through the bitumen-filled pores. There is not a sharp step-change decline in the concentration of solvent at the apparent mobilized live oil film–bitumen interface. The low solvent concentration beyond this interface makes the bitumen more of an “immobile live oil” phase rather than a “raw bitumen” phase. It means that at this low value of solvent concentration and relatively low local temperature, this layer of oil still remains immobile. This immobile live oil phase attains enough mobility upon further solvent and thermal energy propagation within this oil region as time goes on and will eventually drain under the action of gravity later on.

Figure 16c schematically shows the solvent concentration profile in a typical SAGD process. It is obvious that the concentration of solvent in the injected feed stream is zero. In addition, the mobilized oil solvent concentration at the mobilized region–steam chamber interface ($\omega_{\text{Sol}}^{\text{LO}}|_{\text{mobilized_region-S}} = 0$) as well as its corresponding value at the bitumen–mobilized region interface ($\omega_{\text{Sol}}^{\text{LO}}|_{\text{b-mobilized_region}} = 0$) is zero.

Figure 16d also demonstrates the mole fraction profile for the steam and the solvent vapor at a distance close to the interfacial region between the vapor chamber and the mobilized region at a typical SA-SAGD process. Assuming complete mixing of steam and solvent vapor through the invaded region, there would be no solvent concentration gradient within the swept region except for the near interfacial region. It is clear that the mole fraction of either steam or solvent does not change with position when it is far away from the vapor chamber–mobilized region interface where the temperature is constant. Due to the decreasing trend of the temperature profile in the vicinity of the vapor chamber–mobilized region interface, the mole fraction of steam in the gaseous phase decreases while approaching this interfacial region (i.e., position “b” in Figure 16d); however, there is a significant increase in the mole fraction of solvent in the vapor phase in the vicinity of this live oil interface.

(d.2) *Diffusion Mechanism of Mass Transfer in the SA-SAGD Process at the Pore-Scale.* Due to the abrupt solvent concentration gradient at the interfacial region of the SA-SAGD process, mass transfer could take place by molecular diffusion. As the solvent vapor diffuses into the bitumen, a thin film of the live oil phase becomes mobilized. The viscosity of this live oil film is reduced further by the action of thermal diffusion and convection. The draining live oil then engulfs some bubbles of the entrapped nonwetting phase as a result of several pore-scale mechanisms associated with the SA-SAGD process which were demonstrated earlier in Figures 13 and 15. By focusing on the size and shape of these enclosed bubbles, gradual volume shrinkage and possible disappearance along their drainage path is observed. The pore-scale shrinkage/disappearance phenomenon demonstrates the extent of local heat and mass transfer processes. The entrapped gas bubbles

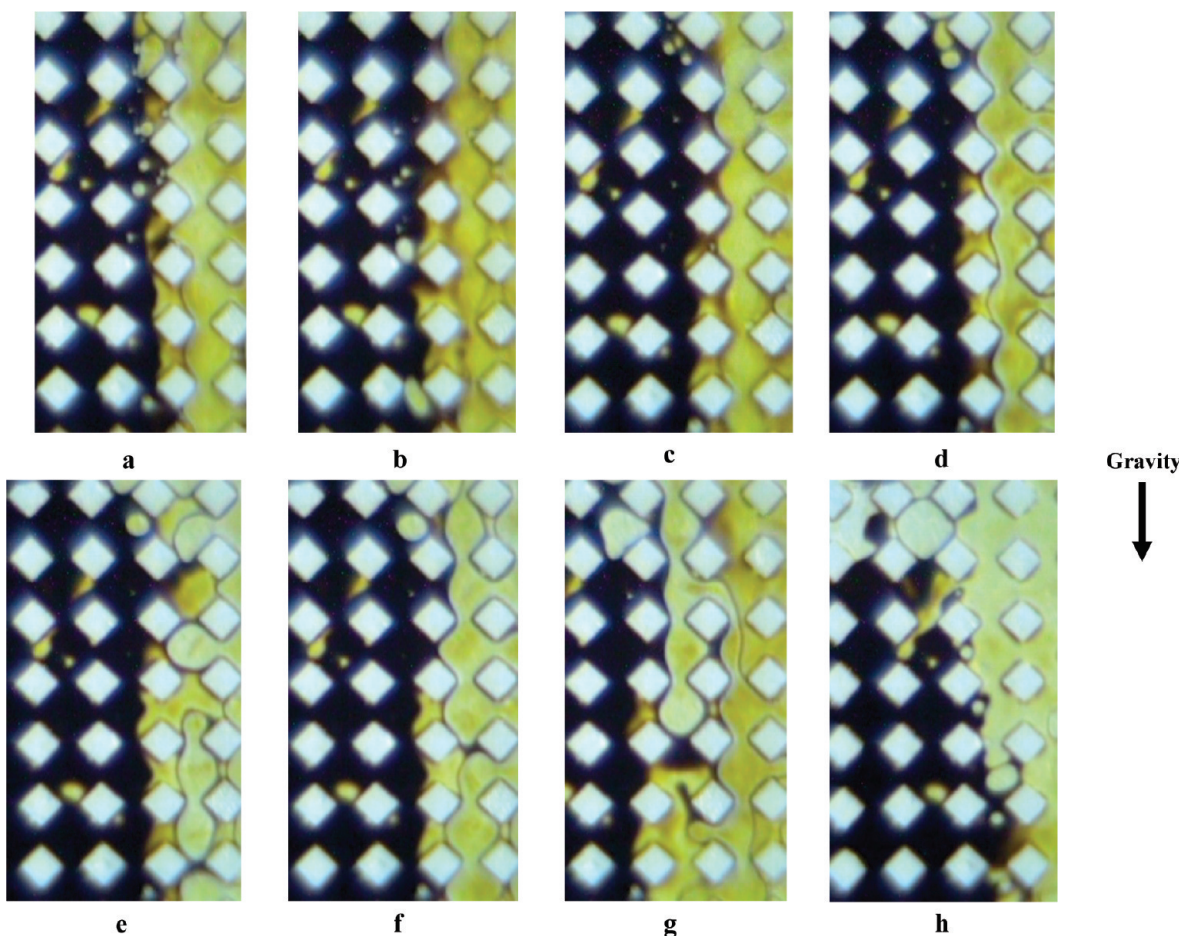


Figure 17. Pore-scale stripping of the bitumen phase by the solvent condensate is evidence of the convective mass transfer mechanism during the SA-SAGD process (DL-1 micromodel, *n*-hexane as the steam additive at 15 vol %, vapor injection temperature of 103.45 °C, time interval 430 s).

tend to disappear with time, which indicates that the local diffusion process enables the complete solubility of the gas pocket into the surrounding live oil continuum. In the SA-SAGD process, it is unlikely to observe pure solvent vapor pockets entrapped within the continuum of the live oil because the limited mole fraction of the injected solvent within the carrying steam phase tends to form a relatively homogeneous gas mixture. The gradual volume shrinkage process of the entrapped gas bubbles, which is more likely to happen based on the visualization experiments of the SA-SAGD process, indicates the process of condensation of the gaseous mixture at the pore-level happens simultaneously with the diffusion mass transfer process of the solvent phase into the live oil. If a sufficiently long drainage path is provided for the entrapped bubbles of the gas mixture, neglecting the chance of coalescence of these propagated bubbles by assuming that the isolated bubbles are independent of each other and remain isolated during their entire drainage path, they would likely be fully converted into small isolated droplets of water condensate down gradient. These phenomena result in the formation of the *in situ* water-in-oil emulsion phase. The volume shrinkage phenomenon of the isolated condensate droplets due to the local diffusion mass transfer was presented through a series of pore-scale events in Figure 14.

(d.3) *Convection Mechanism of Mass Transfer in the SA-SAGD Process at the Pore-Scale.* In the SA-SAGD recovery scheme, the convective mass transfer process is expected to play an important role in the overall mass transfer scheme

when the solvent phase is allowed to condense at the bitumen interface. It is evident that the condensed solvent phase, flowing over the nominal SA-SAGD interface, strips-off the bitumen phase while draining down gradient by a combination of capillary, convective mass and heat transfer phenomena. The presence of a temperature gradient near the interfacial region, which is as a result of the steam condensation within the invaded region, results in improved bitumen recovery because of the enhanced convection mass transfer from solvent condensate to bitumen. The liquid solvent washes away the bitumen-filled pores or pores which are partially filled with bitumen either from top-side, bottom-side, or sideways in the direction of gravity. The draining liquid solvent not only strips the bitumen off the bitumen-filled pores, but it also helps to enhance the mixing process of the live oil and the solvent phase at the pore-scale. This was verified clearly in the videos taken from the pore-level phenomena of the SA-SAGD process during the course of the visualization experiments when the draining solvent condensate phase has a lot of bitumen striations running through it. A nearly perfect vertical interface was observed between the liquid solvent and the bitumen at the pore scale when liquid solvent was flowing all over the bitumen-filled pores. The near flat interface, which is extended through the middle of the pore bodies, is an indication of the extent of miscibility of the acting phases at the pore-level due to higher solvent concentration near the interface. One can clearly distinguish between the flat interface of the liquid solvent-bitumen fluid pair and the curved interface of the solvent vapor-live oil fluid pair at the

pore-scale. Figure 17 contains a series of pore-scale snapshots starting from the top left and ending at the bottom right showing that the bitumen phase is stripped away from the bitumen-saturated pores by continuous flow of excess liquid solvent. The presence of a smooth interface at the microlevel is also observed.

(e) Asphaltene Precipitation during the SA-SAGD Process at the Pore-Scale. Asphaltene is the nonvolatile end of the asphaltenic crude oil. It has polar molecular characteristics of aromatic structure and often contains heavy metals and nitrogen. Asphaltene is defined as the insoluble fraction of the crude oil in excess volume of normal alkanes such as normal pentane and normal heptane, but soluble in excess volume of other solvents such as benzene and toluene at room temperature and atmospheric pressure. Several factors influence the onset of asphaltene flocculation and precipitation from an asphaltenic crude oil in a displacement process, namely temperature, pressure, and compositional changes. However, the temperature has a weaker effect on the asphaltene precipitation. It is believed that temperature change may weakly affect the process of asphaltene flocculation and may enhance or inhibit the overall precipitation process. An increase in the concentration of light chain hydrocarbons, such as *n*-pentane and *n*-heptane in the excess volume can profoundly enhance the asphaltene precipitation process.³⁵ Asphaltene precipitates out of the heavy oil and bitumen if the phase equilibrium between the components is disturbed according to operating conditions. Asphaltene precipitation has a profound effect on the viscosity reduction of the heavy oil. The deasphalting process of the heavy oil and bitumen, which could be an induced phenomenon during the course of any condensing solvent aided process of heavy oil recovery at the pore-scale, could upgrade the heavy oil *in situ* to the extent of reducing its inherent viscosity by several orders of magnitude. Asphaltene precipitation was observed during the course of the VAPEX process with propane as the solvent when the operating pressure was above the dew point of propane.²⁸ It was concluded that the propane liquid to oil ratio was required to be greater than 0.35 by mass in order to experience asphaltene precipitation. While *in situ* asphaltene precipitation reduces the operating and environmental expenses of thermally or catalytically upgrading processes of the heavy oil and bitumen, some people think that it will reduce the permeability and may have an adverse impact on the oil production as well as the sweep efficiency. Some also think that low inherent permeability values of the formation may be problematic for implementing solvent processes because if asphaltene precipitates, it may drastically reduce the permeability or plug the formation. As was presented previously,^{24,25} it is unlikely to experience asphaltene precipitation during the SAGD process at the pore-level based on our visualization experiments. In other words, steam heating of the bitumen phase within the temperature range of 100–130 °C did not destabilize the asphaltene content of the bitumen to the extent of its precipitation. However, the extent of asphaltene precipitation was more pronounced during the course of the SA-SAGD process, especially when the solvent was allowed to condense ahead of the nominal SA-SAGD interface. In these cases, the swept region contains vertical striations of the precipitated asphaltene where liquid solvent was in contact with bitumen. There were still some localized spots within the invaded region in which limited-length residual oil ganglia were present within the pore bodies ahead of the apparent SA-SAGD interface without any sign of extensive asphaltene precipitation.

As the main drainage driving force of the SA-SAGD process is based on the gravity force, we were interested in

studying the impact of asphaltene precipitation on vertical permeability reduction of the porous media. From our visualization studies of the SA-SAGD process, it turns out that asphaltene could precipitate out of the continuous bitumen phase as soon as it is subjected to the excess liquid solvent. The precipitated asphaltene can block the pore constrictions as well as randomly selected pore bodies in a homogeneous structure to the extent of eliminating fluid flow near the blocked region. The gaseous mixture has to reroute in order to reach the bitumen phase, and the draining phases could no longer drain through those clogged flow paths (Figure 18a and b). However, it is clear that the pore blockage is not a permanent issue for most of the clogged flow pathways in the SA-SAGD operation as the injected fresh gaseous mixture could open up the blocked pore constrictions and pore bodies, hence creating randomly propagated zigzag flow paths through the blocked region. These openings would remain as accessible flow pathways for the gaseous mixture ahead of the nominal SA-SAGD interface within the swept region, providing continuous flow of steam and solvent toward the bitumen region (Figure 18d). On the other hand, the mobilized asphaltene particles, in the form of fine particles, drain toward the production end along with the stream of the draining liquids. One of the drawbacks of the fine migration of the mobilized asphaltene particles is the production line blockage as a result of fine build up at the production well (Figure 18c).

The precipitation of asphaltene, however, limits the drainage of liquid phases through the mobilized region temporarily. The chance of pore-scale mixing of the excess liquid solvent within the oil and potential of subsequent asphaltene precipitation and local blockage of the draining pathways exists. The frequent reshaping of the draining liquid phases while draining within the pores which have been already blocked partly by the precipitated asphaltene is an evidence of the effect of asphaltene precipitation on the scheme of fluid flow through porous patterns, so is the frequent resizing of the draining liquid phases as a result of capillary phenomenon of snap-off mechanism when moving past the clogged section of the pores. Considering the low concentration of solvent vapor in the injected gaseous mixture, which is in the order of 5–15 vol %, and presented observations regarding asphaltene precipitation at 15% volume content of the feed stream to be solvent vapor, it is apparent that there is no need for high solvent content in the injected gaseous mixture to induce *in situ* upgrading of the crude in the form of asphaltene precipitation. The condensing nature of the solvent phase at the pore level, even at low solvent content values of the gaseous mixture in the SA-SAGD process, guarantees asphaltene precipitation and possible *in situ* upgrading. The extent of *in situ* upgrading is more severe in the case of the SA-SAGD process compared to that of the conventional VAPEX process, even at higher live oil solvent compositions in the conventional VAPEX process (i.e., 48% with *n*-pentane and 38% with butane^{26,34,36}). It seems that although the solvent content of the produced live oil is lower in the SA-SAGD process compared to that of the VAPEX process, the localized pore-scale liquid solvent concentration in the condensing mode of the SA-SAGD process is high enough to promote asphaltene precipitation. In order to review the process of asphaltene precipitation within the mobilized region of the SA-SAGD process, it would be beneficial to address the schematic diagrams presented in Figures 16b. As was described before, the solvent concentration changes abruptly from its initial value at the gaseous mixture which is the vapor solvent concentration at the invaded area far

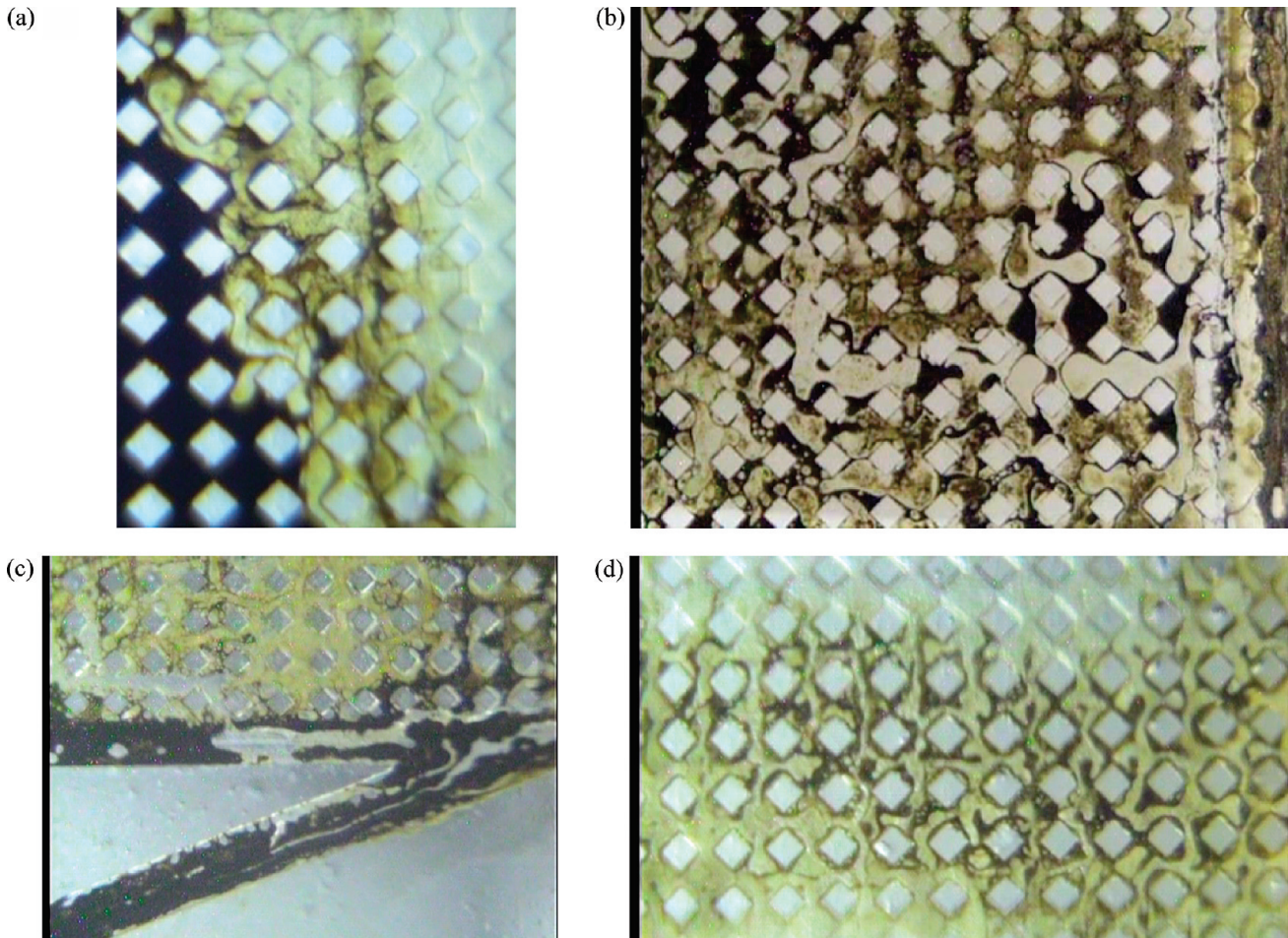


Figure 18. State of in situ asphaltene precipitation as a result of excess solvent condensate near the interfacial region of a typical SA-SAGD process. (a) Asphaltene precipitated at the pore-scale within the mobilized region which caused reshaping/resizing of the phases flowing past it (OM-2 micromodel, *n*-hexane as the steam additive at 15 vol %, vapor injection temperature of 101.45 °C, time 7845 s). (b) Severe asphaltene precipitation within the mobilized region which prevents the gravity drainage process because of the impaired vertical permeability (OM-1 micromodel, *n*-hexane as the steam additive at 15 vol %, vapor injection temperature of 101.85 °C, time 8615 s). (c) Blockage of the production line as well as down-structured pore space as a result of asphaltene mobilization in the form of fine migration (DL-1 micromodel, *n*-pentane as the steam additive at 15 vol %, vapor injection temperature of 102.75 °C, time 8455 s). (d) Asphaltene precipitation within the invaded region, followed by reopening of pores via flow paths due to gas phase invasion through the blocked region (DL-1 micromodel, *n*-pentane as the steam additive at 15 vol %, vapor injection temperature of 102.15 °C, time 8230 s).

from the gaseous phase-mobilized region interfacial area, to zero at the raw bitumen side through a series of pore-scale sections called the mobilized region and the mobilized live oil film. The mobilized region composes of 1–5 pores in thickness, behind which the mobilized live oil film with the thickness of 1–2 pores drains over the pores filled with the solid bitumen phase. The bitumen content of these pores might contain a low level of solvent concentration in it and, therefore, could not be considered as the raw bitumen. However, this solvent content is not to the extent at which it could mobilize the bitumen in the direction of gravity and hence the bitumen could not be considered as the mobilized live oil. The depth of the mobilized live oil film is between 1 and 2 pores in thickness over which the solvent content of the live oil would be reduced from $\omega_{\text{Sol}}^{\text{LO}}|_{\text{mobilized_region-LO}}$ to $\omega_{\text{Sol}}^{\text{LO}}|_{\text{b-LO}}$, and the latter is not necessarily zero as there might be some immobile live oil behind the mobilized live oil film. At the mobilized live oil film–bitumen interface, there is still some minor solvent concentration gradient which could lead to solvent diffusion through the bitumen phase. Excess liquid solvent near the nominal SA-SAGD

interface could cause asphaltene precipitation ahead of the nominal SA-SAGD interface toward the swept region, especially within the mobilized region.

Conclusions

A series of flow visualization experiments were conducted using glass micromodels to mechanically investigate the pore-scale aspects of the SA-SAGD process. This visualization study indicates that

- Periodic condensation of steam and solvent at the nominal SA-SAGD interface causes condensate build up ahead of the nominal vapor–liquid interface, indicative of the local heat transfer mechanism of the process at the pore-level. Direct drainage displacement of this condensate by the invading gaseous phase enhances local pore-scale mixing within the mobilized region ahead of the nominal SA-SAGD interface. Moreover, mobilized-oil filled pores are cleaned up by a combination of direct drainage displacement of oil by condensate as well as by gas phase, and film-flow drainage mechanism.

- Asphaltene precipitation was found to be a temporary phenomenon at the pore-scale due to the local convective mixing as well as partial reopening of the clogged pores by the injected vapor phase.
- Simultaneous flow of steam, solvent vapor, condensate phase, and mobilized oil was observed within the mobilized region, ahead of the apparent SA-SAGD interface. The gas phase could be considered as the only truly nonwetting phase during this gravity drainage process.
- Periodic formation and rupture of the oil films within the invaded area and the mobilized region results in complete oil mobilization with very small amount of residual oil phase within the vapor-invaded zone.
- Local heat transfer mechanisms include conduction and convection. Enclosed gas bubbles and engulfed condensate droplets within the continuum of the live oil are responsible for the convective element of the heat transfer at the pore level.
- Mass transfer at the pore-scale occurs by diffusion mass transfer as well as convective mass transfer caused by capillary displacement mechanism and flow by gravity drainage.

Acknowledgment. The financial support of this research provided by the Natural Sciences and Engineering Research Council of Canada (NSERC) is gratefully acknowledged. The authors would like to express their gratitude to the Micro-Electronics and Heat Transfer Laboratory (MHTL), University of Waterloo, especially Professor Richard Culham (MHTL director) and Professor Pete Teertstra, for providing continuous support during the course of the visualization studies. The authors thank the kind support of Professor M. B. Dusseault for providing the oil samples.

Nomenclature

Variables

T = temperature (°C)

y = mole fraction in the vapor phase

Greek Letters

δ = pore-scale thickness

ω = solvent concentration

Subscripts

m = mobilized region

Solvent = solvent phase

$LO-V$ = interface between the mobilized live oil film and the vapor-invaded pores

$b-LO$ = interface between the bitumen-filled pores and the mobilized live oil film

$mobilized_region-V$ = interface between the mobilized region and the vapor-filled pores

$LO-mobilized_region$ = Interface between the mobilized live oil film and the mobilized region

$mobilized_region-S$ = interface between the mobilized region and the steam-invaded pores

$b-mobilized_region$ = interface between the bitumen-saturated pores and the mobilized region

Steam = steam phase

Superscripts

* = mobilized live oil film

LO = live oil